

SLOT – BASED BANDPASS FILTER AND DIRECTIONAL COUPLER

CHUAH LYE SING

**A project report submitted in partial fulfilment of the
requirements for the award of the degree of
Bachelor (Hons) of Electronic and Electrical Engineering**

**Faculty of Engineering and Science
Universiti Tunku Abdul Rahman**

September 2012

DECLARATION

I hereby declare that this project report is based on my original work except for citations and quotations which have been duly acknowledged. I also declare that it has not been previously and concurrently submitted for any other degree or award at UTAR or other institutions.

Signature : _____

Name : CHUAH LYE SING

ID No. : 09UEB04671

Date : _____

APPROVAL FOR SUBMISSION

I certify that this project report entitled “**SLOT – BASED BANDPASS FILTER AND DIRECTIONAL COUPLER**” was prepared by **Chuah Lye Sing** has met the required standard for submission in partial fulfilment of the requirements for the award of Bachelor of Electronic and Electrical Engineering (Hons.) at Universiti Tunku Abdul Rahman.

Approved by,

Signature : _____

Supervisor: Dr. Lim Eng Hock

Date : _____

The copyright of this report belongs to the author under the terms of the copyright Act 1987 as qualified by Intellectual Property Policy of University Tunku Abdul Rahman. Due acknowledgement shall always be made of the use of any material contained in, or derived from, this report.

© 2012, Chuah Lye Sing. All right reserved.

Specially dedicated to
my beloved parents and all friends.

ACKNOWLEDGEMENTS

I would like to thank my supervisor, Dr Lim Eng Hock, for his valuable advice and guidance throughout all the stages of this research project. His stimulating conversation and discussion have been a constant source of valuable ideas in the development of these new devices. He is always ready to give consultation all the time. He is always ready to give help when I get any problems in this project.

In addition, I would like to acknowledge to my seniors and friends who are and have been doing their research under the supervision same with me, Dr Lim. They have shared their knowledge and experience with me and are willing to render a helping hand whenever I faced problems.

I would like to thank UTAR for preparing such a good environment for me. Besides that, I am thankful to the laboratory assistants who helped me throughout the research project.

SLOT – BASED BANDPASS FILTER AND DIRECTIONAL COUPLER

ABSTRACT

Directional coupler is a four-port device that couples the input power at Port 1 to Port 2 (Through Port) and Port 3 (Coupled Port), but not to Port 4 (Isolation Port). Since the directional coupler is a linear device, any port can be input port but the through, coupled and isolation port will be change too. Nowadays, directional coupler and bandpass filter are almost used in all communication systems. They play an important role in the monitoring and measurement of signal samples within an assigned operating frequency. The first part of project is to propose a slot-based directional coupler with high performance which operation in certain frequency. By used High Frequency Structure Simulator (HFSS) to simulate and optimize the amplitude of the directional coupler. After that, the proposed directional couplers are fabricated on RT Duroid 5870 substrate and measured using the Vector Network Analyzer (VNA) in the laboratory. Finally, the simulation and experimental results are compared, showing either the result good in agreement or not. Case studies have been conducted on the proposed directional couplers in order to study the effects of different design parameters. Discussion and recommendations have been made after each case study. For second part, a slot-based bandpass filter with controllable transmission zero is presented. The proposed bandpass filter has simulated by using HFSS and parametric analysis has been done. Discussion and conclusion have been made after each case study.

TABLE OF CONTENTS

DECLARATION	ii
APPROVAL FOR SUBMISSION	iii
ACKNOWLEDGEMENTS	vi
ABSTRACT	vii
TABLE OF CONTENTS	viii
LIST OF TABLES	xi
LIST OF FIGURES	xii
LIST OF SYMBOLS / ABBREVIATIONS	xvi

CHAPTER

1	INTRODUCTION	1
	1.1 Background	1
	1.2 Issues	4
	1.3 Research Aim and Objectives	5
	1.4 Project Motivation	6
	1.5 Thesis Overview	7
2	LITERATURE REVIEW	8
	2.1 Background	8
	2.2 Directional Coupler	8
	2.2.1 Theory of Directional Coupler	9
	2.3 Bandpass filter	13
	2.3.1 Theory of Bandpass filter	13

2.4	Recent Developments	15
2.4.1	Microstrip Directional Coupler Loaded With Shunt Inductors	15
2.4.2	Transmission line Directional Couplers for Impedance Transforming	18
2.4.3	Novel Trigonal Dual-mode Filter	22
2.4.4	Microstrip Band-pass Filter With Slotted Hexagonal Resonators and Capacitive Loading	24
2.5	Introduction of Simulation Tools	26
2.5.1	High Frequency Structure Simulator	26
2.5.2	TX-Line Calculator	27
3	SLOT-BASED DIRECTIONAL COUPLER	28
3.1	Background	28
3.2	Configuration	28
3.3	Simulation	31
3.4	Parametric Analysis	32
3.5	Results	48
3.6	Discussion	49
4	SLOT-BASED BANDPASS FILTER	51
4.1	Background	51
4.2	Configuration	51
4.3	Simulation	53
4.4	Parametric Analysis	54
4.5	Discussion	75
	FUTURE WORK AND RECOMMENDATIONS	76
5.1	Achievements	76
5.2	Future Work	77
5.3	Conclusion	77

REFERENCES

LIST OF TABLES

TABLE	TITLE	PAGE
1.1	Frequency band designation.	2
2.1	Port definition of directional coupler.	10
3.1	Comparison of the experiment and HFSS simulation results	49

LIST OF FIGURES

FIGURE	TITLE	PAGE
1.1	Summary of the history of wireless system.	2
1.2	General microstrip structure.	5
2.1	Power flows in conventional directional coupler.	9
2.2	Power flows in directional coupler with port3 as input port.	9
2.3	Single section quarter-wavelength directional coupler.	13
2.4	Bandwidth measured of the Band-pass filter.	14
2.5	Schematics of a conventional microstrip directional coupler.	16
2.6	Schematics of the proposed microstrip directional coupler with shunt inductors.	16
2.7	Prototype of the 20-dB directional coupler with shunt inductors.	16
2.8	S-parameters of the directional coupler with shunt inductors.	17
2.9	Directivity and coupling levels of directional coupler with shunt inductors.	17
2.10	Even mode equivalent circuit.	18
2.11	Odd mode equivalent circuit.	19
2.12	Prototype of the proposed directional coupler.	21

2.13	Measured results compared with simulation ones.	21
2.14	Layouts of the proposed trigonal dual-mode filter with capacitive S-L coupling.	22
2.15	Prototype of trigonal dual-mode filter.	23
2.16	Simulated and measured frequency responses of the filter.	23
2.17	Layout of the hexagonal filters.	24
2.18	Prototype of the proposed filter.	25
2.19	Measured results of the proposed filter.	25
3.1	Configuration of the proposed microstrip slot-based directional coupler.	29
3.2	Prototype of the top view of the proposed slot-based directional coupler.	30
3.3	Prototype of the bottom view of the proposed slot-based directional coupler.	30
3.4	S-parameter of the proposed slot-based directional coupler.	32
3.5	Effect of length l_1 on the slot-based directional coupler.	33
3.6	Effect of length l_2 on the slot-based directional coupler.	34
3.7	Effect of width w_1 & w_2 on the slot-based directional coupler.	35
3.8	Effect of width w_1 on the slot-based directional coupler.	36
3.9	Effect of width w_2 on the slot-based directional coupler.	37
3.10	Effect of width w_3 on the slot-based directional coupler.	38
3.11	Effect of gap g_1 on the slot-based directional coupler.	39

3.12	Effect of gap g_2 on the slot-based directional coupler.	40
3.13	Effect of gap g_3 on the slot-based directional coupler.	41
3.14	Effect of gap g_4 on the slot-based directional coupler.	42
3.15	Effect of gap g_5 on the slot-based directional coupler.	43
3.16	Effect of distance d_1 on the slot-based directional coupler.	44
3.17	Effect of distance d_2 on the slot-based directional coupler.	45
3.18	Effect of distance d_3 on the slot-based directional coupler.	46
3.19	Effect of distance d_4 on the slot-based directional coupler.	47
3.20	Simulated and measured amplitude responses of the slot-based directional coupler.	48
4.1	Top-down view of the proposed slot-based bandpass filter.	52
4.2	Simulated result of the proposed slot-based bandpass filter.	54
4.3	Effects of gap g_1 on the slot-based bandpass filter.	55
4.4	Effects of gap g_2 on the slot-based bandpass filter.	56
4.5	Effects of gap g_3 on the slot-based bandpass filter.	57
4.6	Effects of gap g_4 on the slot-based bandpass filter.	58
4.7	Effects of gap g_5 on the slot-based bandpass filter.	59
4.8	Effects of width w_1 on the slot-based bandpass filter.	60
4.9	Effects of width w_2 on the slot-based bandpass filter.	61

4.10	Effects of width w_3 on the slot-based bandpass filter.	62
4.11	Effects of distance d_1 on the slot-based bandpass filter.	63
4.12	Effects of distance d_2 on the slot-based bandpass filter.	64
4.13	Effects of length l_1 on the slot-based bandpass filter.	65
4.14	Effects of length l_2 on the slot-based bandpass filter.	66
4.15	Effects of length l_3 on the slot-based bandpass filter.	67
4.16	Effects of length l_4 on the slot-based bandpass filter.	68
4.17	Effects of length l_5 on the slot-based bandpass filter.	69
4.18	Effects of length l_6 on the slot-based bandpass filter.	70
4.19	Effects of length l_7 on the slot-based bandpass filter.	71
4.20	Effects of length l_8 on the slot-based bandpass filter.	72
4.21	Effects of length l_9 on the slot-based bandpass filter.	73
4.22	Effects of length l_{10} on the slot-based bandpass filter.	74

LIST OF SYMBOLS / ABBREVIATIONS

λ	Wavelength, m
f	Frequency, Hz
c	Speed of light, m/s
ϵ_r	Dielectric constant
ϵ_{eff}	Effective dielectric constant
h	Thickness of substrate, mm
w	Width of microstrip lines, mm
Z_o	Characteristic impedance, Ω
Z_{in}	Input impedance, Ω
S_{11}	Reflection coefficient, dB
S_{21}	Insertion loss, dB
S_{31}	Insertion loss, dB
S_{41}	Isolation, dB

CHAPTER 1

INTRODUCTION

1.1 Background

Wireless technologies have been used in pass 100 years ago. The wavelengths of the wireless transmission have been used from the longer to the smaller. Figure 1.1 below show the summary of the history of wireless system. Nowadays, Microwave and radio frequency wireless technologies have been extensively used in many commercial and military applications. These applications include communications, radar, navigation, remote sensing, RF identification, broadcasting, automobiles, and so on. In general, microwave spectrum spreads from 300MHz to 300 GHz, which corresponds to a wavelength ranging from 1mm to 1m. Table 1.1 shows the frequency band designation. Furthermore, passive components like filter, power divider, coupler and circulator are common used in microwave technologies.

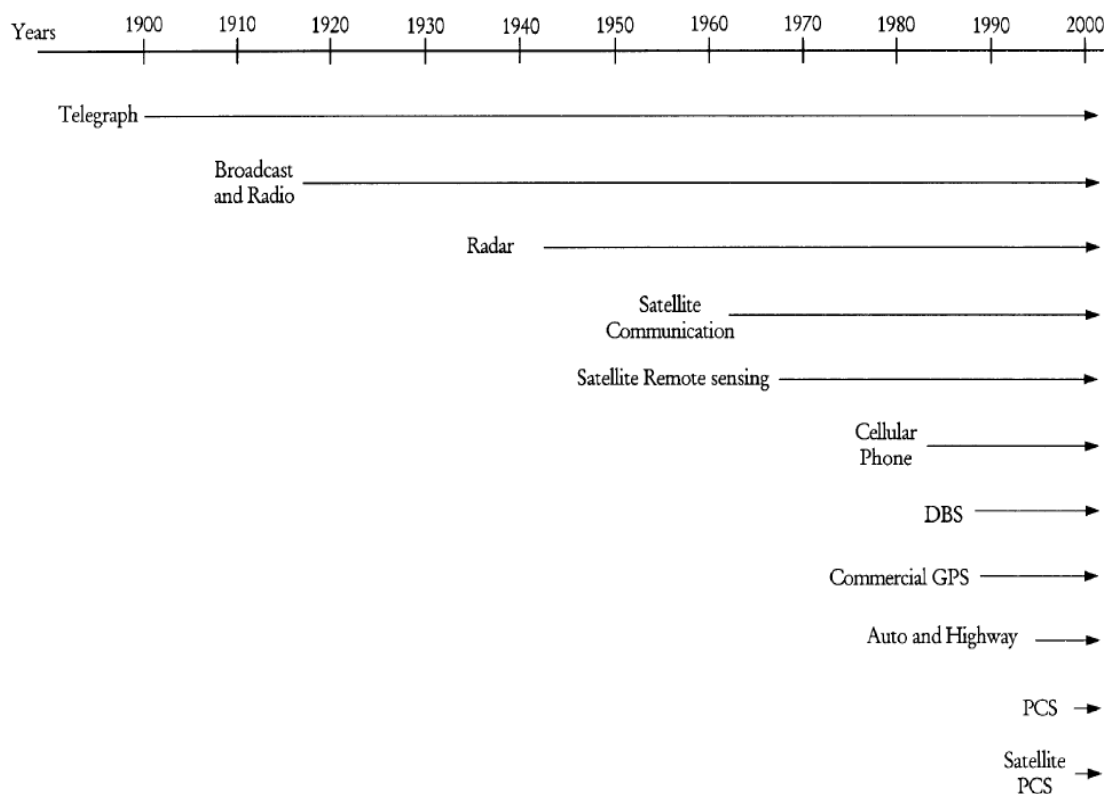


Figure 1.1: Summary of the history of wireless system.

Table 1.1: Frequency band designation.

Band name	Abbr	Band	Frequency	Wavelength	Example uses
Extremely low frequency	ELF	1	3 – 30Hz	100,000km – 10,000km	Communication with submarines
Super low frequency	SLF	2	30 – 300Hz	10,000km - 1000km	Communication with submarines
Ultra low frequency	ULF	3	300 – 3000Hz	1000km – 100km	Communication with underground mines
Very low frequency	VLF	4	3 – 30kHz	100km – 10km	Submarines communication, avalanche beacons, wireless heart rate monitor, and geophysics

Low frequency	LF	5	30 – 300kHz	10km - 1km	Navigation, time signals, AM Radio
Medium frequency	MF	6	300 – 3000kHz	1km - 100m	AM Radio
High frequency	HF	7	3 – 30 MHz	100m – 10m	Shortwave Radio and aviation communication
Very high frequency	VHF	8	30 – 300MHz	10m – 1m	FM Radio, TV broadcasts, and aircraft communication
Ultra high frequency	UHF	9	300 – 3000MHz	1m – 100mm	TV broadcasts, microwave oven, mobile phones, wireless LAN Bluetooth, GPS, and two-Way Radio
Super high frequency	SHF	10	3 – 30GHz	100mm – 10mm	Radars, mobile phones, and commercial wireless LAN
Extremely high frequency	EHF	11	30 – 300GHz	10mm – 1mm	High-speed satellite microwave transmission

Obtained from: <http://globalmicrowave.org/microwaves.php>

From the first telephone generation, human was thinking how to generate a phone without wire. During the World War II, human want to use microwave system to detecting and locating enemy planes and ships. In the recent years, microwave frequencies have come into widespread use in communication system and many other technologies.

In addition, various types of designs and specifications of microwave components are available and can be found on IEEE Xplore database. These publications continue to increase widely. This mean microwave engineering has become more and more important technologies.

1.2 Issues

Directional couplers are passive devices used in the field of radio technology. Generally, couplers are components used for power division or power combining (Pozar, 1998). They have many application, these include; providing a signal sample for measurement or monitoring, feedback, combining feeds to and from antenna, providing taps for cable distributed system such as cable TV, separating transmitted and received signal on telephone lines, balanced mixers, balanced amplifiers, phase shifters, automatic signal level control and many other applications (Wikipedia, 2012). Operating frequency of the directional coupler has been designed according to the different operating function for the systems. If the bandwidth of the directional couplers is more widely, it's more preferable. It's because for wide bandwidth, it allows more component to share the same spectrum simultaneously.

In the 40s, E- and H- plane waveguide tee junctions, the Bethe-hole coupler, multi-hole directional coupler and various types of couplers using coaxial probes were invented and characterized at the MIT Radiation Laboratory (Pozar, 1998). However, in the mid-1950s through the 1960s, many of these directional couplers were reinvented using stripline and microstrip technologies due to its easy implementation and integration. Because of these new technologies developed, it led variety type of dividers and couplers developed, such as the Wilkinson divider, the branch line hybrid and more many type couplers.

Microstrip technology is a type of electrical transmission line which can be fabricated using printed circuit board (PCB) technology. It also can use photolithographic process to fabricate, which is the process use in this project. The reasons to choose microstrip technology in this project because it has many advantages such as lowest cost, small in size, lighter weight, absence of critical matching and cut-off frequency, ease of active device integration (Kai Chang,2000). Figure 1.2 shows the general microstrip structure.

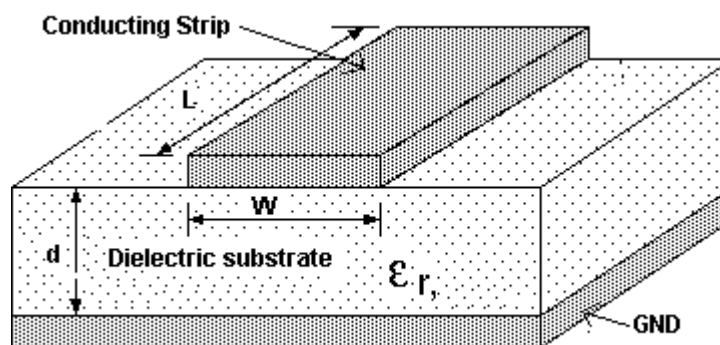


Figure 1.2: General microstrip structure.

Figure 1.2 shows the cross section view of a microstrip. It consists of a conducting strip separated from a ground plane by a dielectric layer known as the substrate. W , L and d represent the width of the strip line, length of the strip line and height of the substrate respectively. Moreover, ϵ_r is the dielectric constant of the substrate. They have several type of substrate, RT Duroid 5870 ($\epsilon_r = 2.33$), RT Duroid 5880 ($\epsilon_r = 2.2$) and other more. Hard substrates have better reliability and lower thermal expansion coefficient but are more expensive and inflexible. In addition, microstrip has major advantages over stripline and waveguide where all the active components can be install on top of the substrate. It is easy to measure the voltage, current or waves on the board.

Besides that, characteristic impedance is one of the factor need to take care when we designing a board. It will affect the reflection coefficient of the input port, S_{11} and is also known as return loss. When the signal has return loss, this mean the signal has loss due to reflection at a discontinuity of a device. To minimize this problem, the characteristic impedance of the microstrip must be equal to the input impedance of the system normally it is 50Ω .

1.3 Research Aim and Objectives

The main objective of this project is to propose and construct a different type resonators directional coupler by using slot-based technology that can offer better

performances. The targets for this project are to develop a stable, high selectivity and wide bandwidth directional coupler.

The first proposed idea is to design a slot-based directional coupler with high selectivity. This is one of the directional coupler with the coupler line are slot-based. It is a new technique to design a four port microstrip directional coupler where to filtering the signal. In this project, RT Duroid 5870 microstrip board has is used to develop this idea.

In the second part, a slot-based bandpass filter has been designed to passes frequencies within a certain range and rejects frequencies outside that range. Second idea also uses the slot-based technique to design a two port microstrip bandpass filter. FR-4 ($\epsilon_r = 4.4$) has is used to develop this band-pass filter.

After done this project, the author has gained better understanding the theory of some of the passive microwave components like directional couplers and bandpass filters. Besides that, the author has more advances in develop part.

1.4 Project Motivation

Nowadays the microwave and RF wireless technologies keep improving and advance, much type of microwave components keep designed out according to the needs of market. To develop a new prototype of directional coupler with high selectivity and wide bandwidth is one of achievement for the author. Same like to develop a new prototype of bandpass filter, it also a good achievement to the author.

Throughout this project, the author has gained improve the information and theory for the microwave component. Besides that, the author easier to explore and solve the problems due the information and solving skills are advance. It gives the

author extra motivation to explore more related on the directional coupler and bandpass filter.

1.5 Thesis Overview

In this thesis, it consist the necessary theory for microwave components which will be presented in Chapter 2. It includes the directional coupler and bandpass filter. It consists of theory, issues, design considerations and recent developments of various types of microwave components. It is also consists some introduced of the simulation software in this chapter.

In Chapter 3 and Chapter 4, a slot-based directional coupler and slot-based bandpass filter will be discussed detail separately. The design considerations and configuration for two ideas are analyzed in these two chapters. Besides that, parameters were also analyzed and compare in these two chapters. Furthermore, the results and performances of the directional coupler and bandpass filter were discussed and compared to those conventional components. Base on the results obtained, the author can make sure the slot-based directional coupler either successful or not.

Lastly, the conclusion and the recommendations for the further studies as well as the improvements on the design of directional coupler and bandpass filter are given in Chapter 5.

CHAPTER 2

LITERATURE REVIEW

2.1 Background

In this chapter, the theory of the conventional directional coupler and bandpass filter will be analyzed. Besides that, some formula of the directional coupler and bandpass filter will be show. Furthermore, few recent developments will be discussed. Lastly, some simulation tool that has been used in this project will be introduced.

2.2 Directional Coupler

Directional couplers is a common passive components used in communication system and other application. Basically, directional couplers are used for power division or power combining. In power division, an input signal is divided by the coupler into two or more signals of lesser power. In power combining, two or more input signal is combined together into one output signal with higher power.

2.2.1 Theory of Directional Coupler

Generally, directional coupler is a four-port device that contains four ports where input port, direct or through port, coupled port and isolation port. When the input signal applied to input port (port 1) then couples power into direct port (port 2) and coupled port (port 3) but not into isolation port (port 4). However, for an ideal directional coupler, any of the port can be input with different through port, coupled port and isolation port which depend to the case. Figure 2.1 and Figure 2.2 shows the power flows in conventional directional coupler and power flows in directional coupler with port 3 as input port.

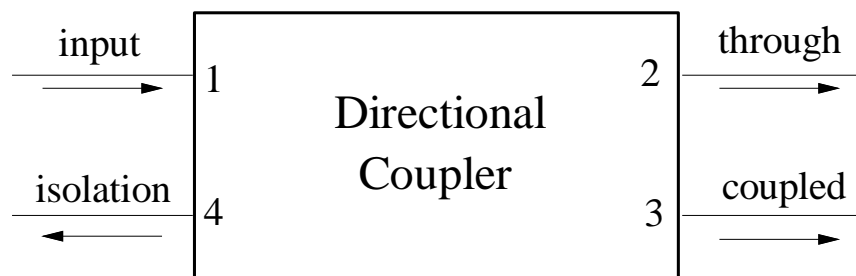


Figure 2.1: Power flows in conventional directional coupler.

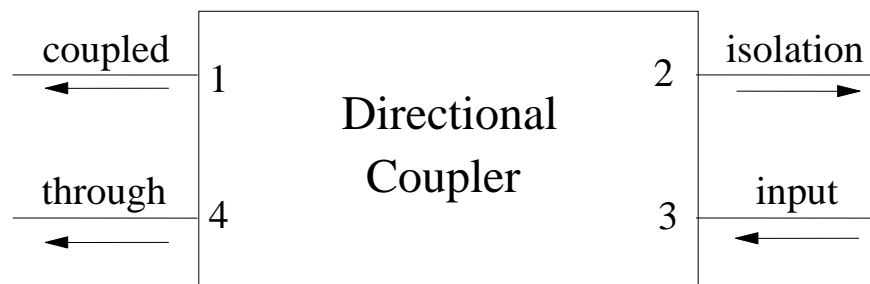


Figure 2.2: Power flows in directional coupler with port3 as input port.

Besides that, we can use scattering matrix of directional coupler to summarize out the port definition of directional coupler. Table 2.1 show the port definition of directional coupler.

Table 2.1: Port definition of directional coupler.

<i>Input</i>	<i>Through</i>	<i>Coupled</i>	<i>Isolation</i>
Port 1	Port 2	Port 3	Port 4
Port 2	Port 1	Port 4	Port 3
Port 3	Port 4	Port 1	Port 2
Port 4	Port 3	Port 2	Port 1

The scattering matrix has the following form:

$$\bar{S} = \begin{bmatrix} 0 & \alpha & j\beta & 0 \\ \alpha & 0 & 0 & j\beta \\ j\beta & 0 & 0 & \alpha \\ 0 & j\beta & \alpha & 0 \end{bmatrix} \quad (1)$$

The ideal coupler is completely characterized by the coupling coefficient c , its re-form as below:

$$\bar{S} = \begin{bmatrix} 0 & \sqrt{1-c^2} & jc & 0 \\ \sqrt{1-c^2} & 0 & 0 & jc \\ jc & 0 & 0 & \sqrt{1-c^2} \\ 0 & jc & \sqrt{1-c^2} & 0 \end{bmatrix} \quad (2)$$

Where $\beta = c$ and $\alpha = \sqrt{1-\beta^2} = \sqrt{1-c^2}$

Furthermore, the coupling coefficient c , will be less than $1/\sqrt{2}$ always. Therefore, we find that:

$$0 \leq c \leq \frac{1}{\sqrt{2}} \quad \text{and} \quad \frac{1}{\sqrt{2}} \leq \sqrt{1-c^2} \leq 1$$

We can re-form it again as below:

$$\bar{S} = \frac{1}{\sqrt{2}} \begin{bmatrix} 0 & 1 & j & 0 \\ 1 & 0 & 0 & j \\ j & 0 & 0 & 1 \\ 0 & j & 1 & 0 \end{bmatrix} \quad (3)$$

From the equation (2): we can define when the signal is given to port, while all other ports are matched. The power flowing out of the port 1 is:

$$p_1^- = |S_{11}|^2 p_1^+ = 0$$

The power coming out of port 2 will become like that:

$$p_2^- = |S_{21}|^2 p_1^+ = (1 - c^2) p_1^+$$

Furthermore, the power coming out of port 3 is:

$$p_3^- = |S_{31}|^2 p_1^+ = c^2 p_1^+$$

Lastly, there is no power flowing out of port 4:

$$p_4^- = |S_{41}|^2 p_1^+ = 0$$

From the scattering matrix above, there have three important parameters in describing the performance of the coupler which are coupling factor, directivity and isolation. (Pozar, 1998) and (Wikipedia, 2012)

Coupling factor (in dB):

- The ratio of input power to the coupled power.

$$C = 10 \log \frac{P_1}{P_3} = -10 \log \frac{P_3}{P_1}$$

Directivity (in dB):

- The ratio of coupled power to the isolated power.

$$D = 10 \log \frac{P_3}{P_4} = -10 \log \frac{P_4}{P_3}$$

Isolation (in dB):

- The ratio of input power to isolated power.

$$I = 10 \log \frac{P_1}{P_4} = -10 \log \frac{P_4}{P_1}$$

However, these also can re-form like this:

$$I = C + D \quad \text{or} \quad D = I - C$$

The directivity should be as high as possible. The directivity is very high at the design frequency and is a more sensitive function of frequency because it depends on the cancellation of two wave components. The coupling factor represents the primary property of a directional coupler. Coupling factor is a negative quantity, it cannot exceed 0dB for a passive device, and in practice does not exceed -3db since more than this would result in more power output from the coupled port than power from the transmitted port and effect their roles would be reversed.

Generally, there are several methods to design a directional coupler. The most common methods to design directional coupler are using coupled-line theory. The coupling level between the ports is due to the interaction of the electromagnetic field along transmission line which has been placed in closely. In addition, it also calls as TEM-mode quarter-wavelength directional coupler. (Leo Young, M.A., Dr.Eng., 1963). Figure below shows the single section quarter-wavelength directional coupler.

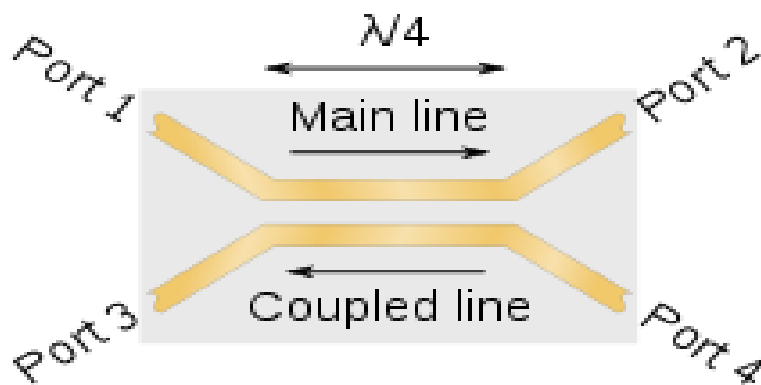


Figure 2.3: Single section quarter-wavelength directional coupler.

Apart from that, waveguide directional couplers, Bethe Hole coupler, and other more also are the methods to design directional coupler.

2.3 Bandpass filter

A bandpass filter is a device that passes frequencies within a certain range and rejects (attenuates) frequencies outside that range. Generally, it used in communication system, amplifier, and other application.

2.3.1 Theory of Bandpass filter

A bandpass filter can be made by cascading together the highpass filter and lowpass filter with the frequency range between the lower and upper -3dB cut-off points being know as the bandwidth of filter. Figure 2.4 shows the bandwidth measured of the bandpass filter.

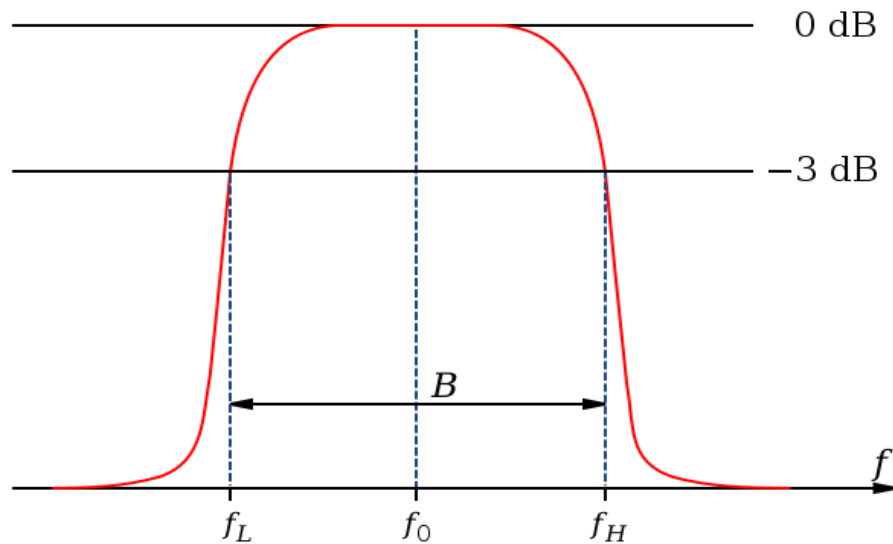


Figure 2.4: Bandwidth measured of the Band-pass filter.

The centre frequency point is the geometric mean of the lower and upper cut-off point which known as lower frequency and upper frequency.

$$\text{CentreFrequency, } f_c = \frac{\text{LowerFrequency, } f_L + \text{HighFrquency, } f_H}{2}$$

An ideal bandpass filter would have a completely flat passband (with no gain or attenuation throughout) and would completely attenuate all frequencies outside the passband. Furthermore, the transition out of the passband would be instantaneous in frequency. However, no bandpass filter is ideal in the practice. The filter does not attenuate all frequencies outside the passband where frequencies are attenuated, but not rejected. It is known as the filter roll-off, and it is normally expressed in dB. Generally, the design of a filter seeks to make the roll-off as narrow as possible, thus allowing the filter to perform as close as possible to its intended design.

2.4 Recent Developments

In order to design directional couplers and bandpass filter with good performance, the author have done some research and reviewed some of the published journals which publish from IEEE Xplore. These published journals are regarding recent developments of directional coupler and bandpass filter.

2.4.1 Microstrip Directional Coupler Loaded With Shunt Inductors

Generally, the parasitic effects of junction discontinuities in various parts of such microstrip directional couplers have critical effects especially on the directivity. So, they should be taken into account. Without proper modelling of these parasitic effects, directivity enhancement becomes extremely difficult especially for weak coupling levels. The demonstrated method of analysis can be applied to obtain exact designs of all previous microstrip directional couplers that are loaded symmetrically with series and/or shunt reactance for directivity enhancement, regardless of the coupling levels. (Seungku Lee, Yongshik Lee, April 2010). The issue of parasitic effects related to junction discontinuities have never been investigated before. Based on the proposed method, a 20dB microstrip directional coupler is designed at 2.4GHz. A maximum directivity of 56dB has been measured, which is an improvement of 48dB over a conventional microstrip directional coupler. Furthermore, 16.3% bandwidth at 2.4GHz has been measured in which the directivity remains above 20dB. (Seungku Lee, Yongshik Lee, April 2010). Therefore, Seungku Lee and Yongshik Lee proposed a microstrip directional coupler loaded with shunt inductors. Below the figure shows the schematics of a conventional microstrip directional coupler and the proposed microstrip directional coupler.

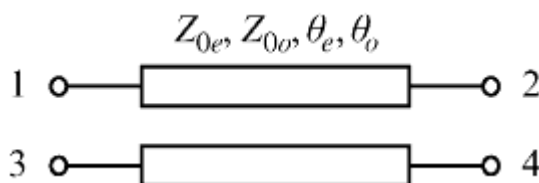


Figure 2.5: Schematics of a conventional microstrip directional coupler.

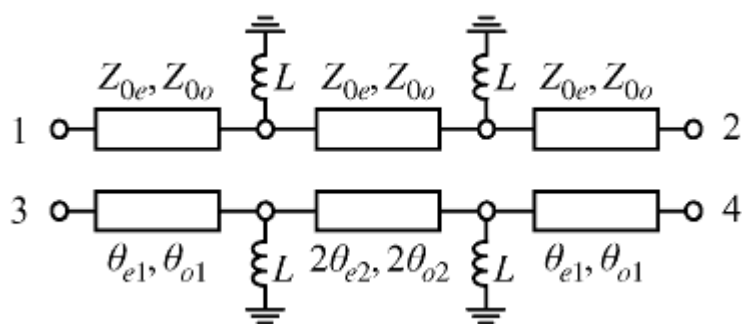


Figure 2.6: Schematics of the proposed microstrip directional coupler with shunt inductors.

For experimental verification, the proposed inductively loaded 20dB directional coupler at 2.4GHz is fabricated in an RF-35 microstrip board with dielectric constant 3.5, thickness of 0.76mm, and 35 μm copper cladding. The inductors are realized with 75 Ω stubs, grounded by via holes of 0.25mm radius. Figure 2.7 show the prototype of 20dB directional coupler with shunt inductor.

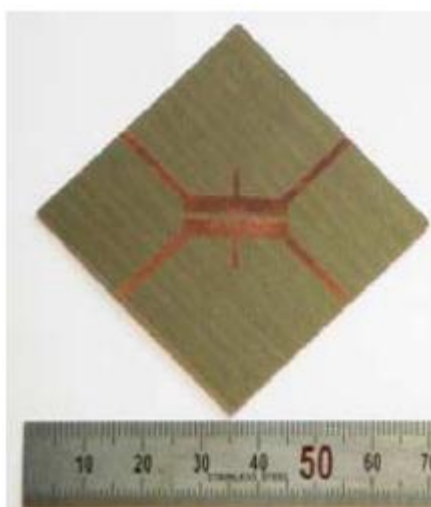


Figure 2.7: Prototype of the 20-dB directional coupler with shunt inductors.

Finally, the fabricated couplers are measured in the 1 to 4GHz range with a MS4624D Vector Network Analyzer from Anritsu. Figure 2.8 shows the full-wave simulated and measured results for the proposed directional coupler. Based on the result shows, a maximum isolation of more than 76dB with coupling level of 20.1dB have been measured at 2.41GHz. The result is in excellent agreement. In addition, figure 2.8 shows the measured and simulated directivity and coupling levels of the proposed and conventional directional coupler.

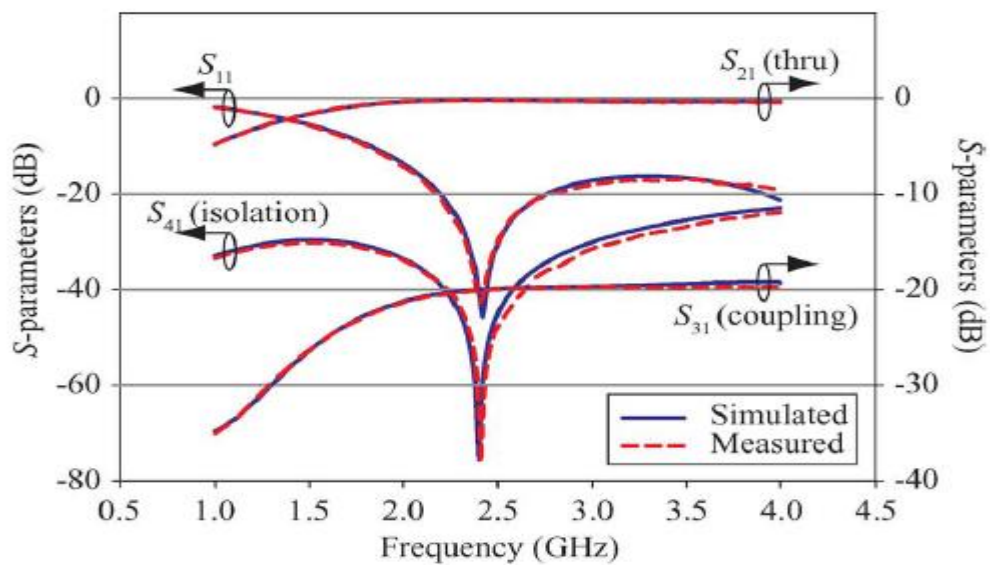


Figure 2.8: S-parameters of the directional coupler with shunt inductors.

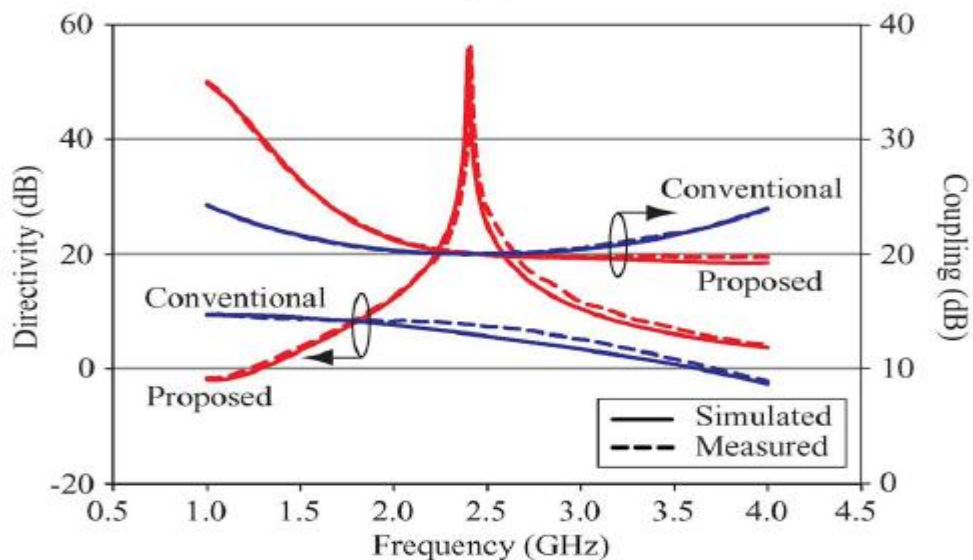


Figure 2.9: Directivity and coupling levels of directional coupler with shunt inductors.

2.4.2 Transmission line Directional Couplers for Impedance Transforming

In this paper, normalized scattering parameters of a two port circuit terminated in arbitrary impedances are derived and design equations of directional couplers for impedance transforming are derived. To verify the design equations, the author a design a microstrip directional coupler with center frequency of 2GHz and fabricated on microstrip circuit board and measured. (Hee-Ran Ahn, Bumman Kim, 2006).

Several theory and applications of the parallel coupled transmission lines are described in many papers. However, they can be applied only for equal termination impedances. In this paper, parallel coupled transmission lines will be analyzed for impedance transforming and design equation of directional couplers will be given.

For the analyses, the scattering parameters of the even and odd mode equivalent circuits are needed to be known. Figure 2.10 and Figure 2.11 shows the even mode equivalent circuit and odd mode equivalent circuit respectively.

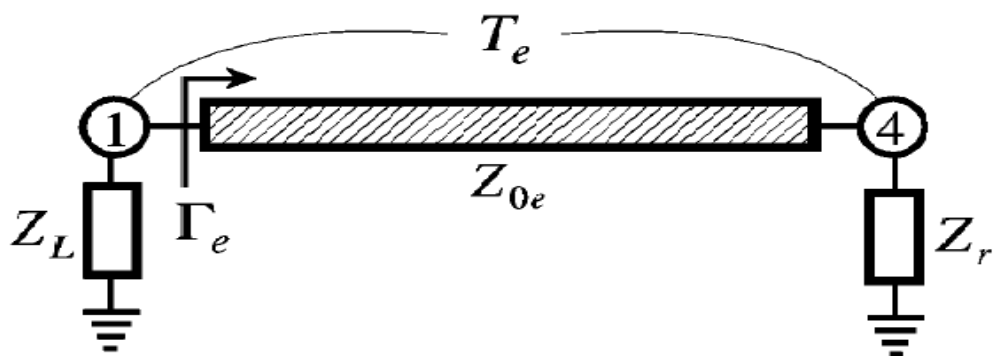


Figure 2.10: Even mode equivalent circuit.

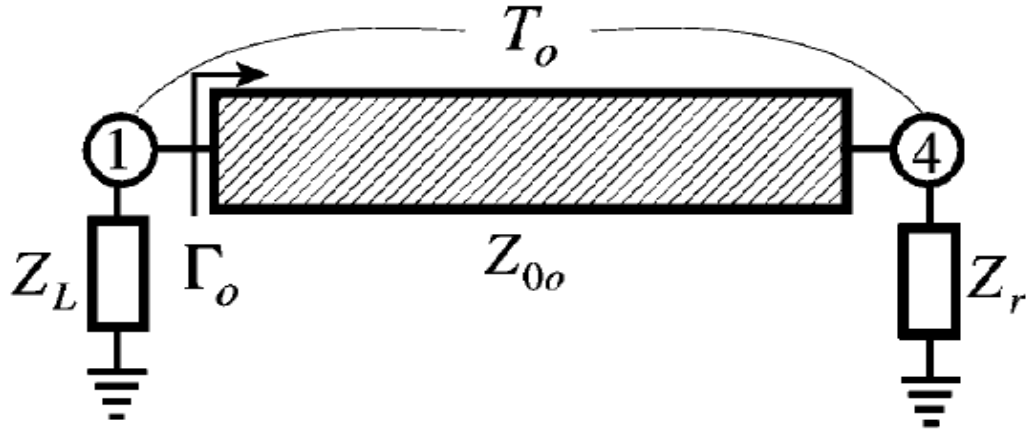


Figure 2.11: Odd mode equivalent circuit.

Using the even and odd mode reflected and transmitted scattering parameters, the reflection coefficient at port 1 obtained as:

$$S_{11} = \frac{2(Z_L - Z_r) \cos \Theta}{2 \left[\cos \Theta (Z_L + Z_r) + j \sin \Theta (Z_{0e} + \frac{1}{Z_{0e}} Z_L Z_r) \right]} + j \frac{\sin \Theta \left(Z_{0e} + Z_{0o} - \left(\frac{1}{Z_{0e}} + \frac{1}{Z_{0o}} \right) Z_L Z_r \right)}{2 \left[\cos \Theta (Z_L + Z_r) + j \sin \Theta \left(Z_{0e} + \frac{1}{Z_{0e}} Z_L Z_r \right) \right]} \quad (1)$$

For matched parallel coupled transmission lines at port1, both real and imaginary parts of S_{11} in above should be zero, which results in:

$$\cos \Theta = 0, \text{ or } \Theta = 90^\circ$$

$$Z_{0e} Z_{0o} = Z_L Z_r.$$

(2)

Applying the matching condition in above to other ports yields:

$$\begin{aligned}
 S_{21} &= \frac{Z_{0e} - Z_{0o}}{Z_{0o} + Z_{0e}} = C \\
 S_{31} &= 0 \\
 S_{41} &= -\frac{j2\sqrt{Z_L Z_r}}{Z_{0o} + Z_{0e}} = -j\sqrt{1 - C^2}
 \end{aligned}
 \tag{3}$$

Based on equation (2) and S_{21} in the equation (3), the required even and odd mode impedances are:

$$\begin{aligned}
 Z_{0e} &= \sqrt{\frac{(1 + C)}{(1 - C)}} Z_L Z_r \\
 Z_{0o} &= \sqrt{\frac{(1 - C)}{(1 + C)}} Z_L Z_r
 \end{aligned}
 \tag{4}$$

Based on the design equation in (4), a microstrip directional coupler with $Z_L = 50\Omega$ and $Z_r = 30\Omega$ was designed at a center frequency of 2GHz, fabricated on a substrate with dielectric constant 3.5 and thickness 30mil. Measurement has been done and compared with simulated result. Figure 2.12 and Figure 2.13 shows the prototype of the proposed directional coupler and measured results compared with simulated ones.

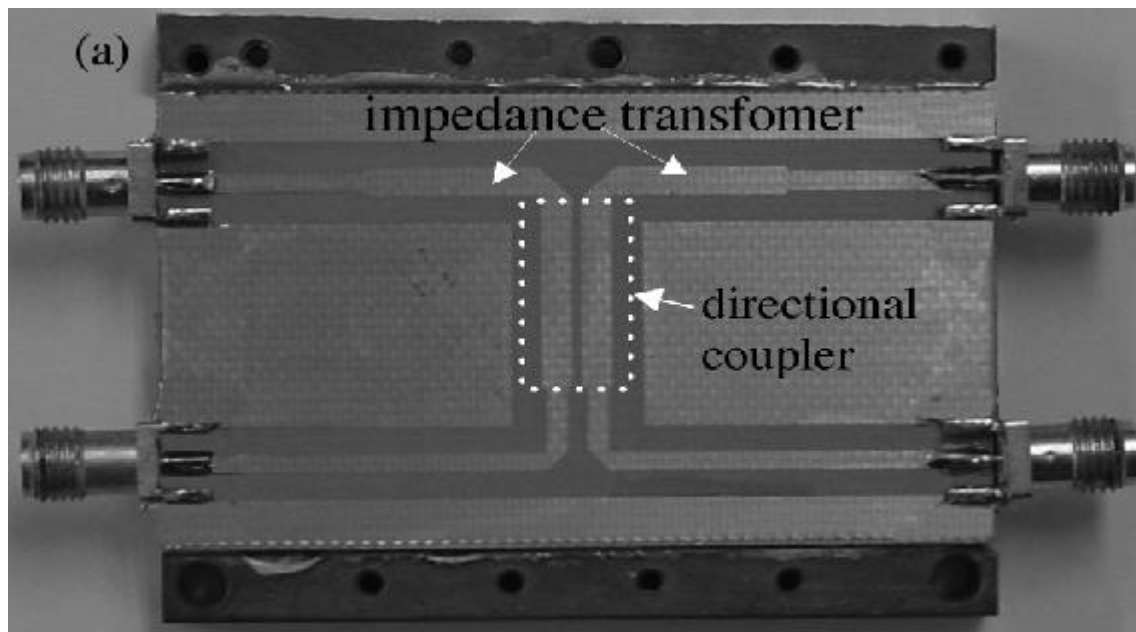


Figure 2.12: Prototype of the proposed directional coupler.

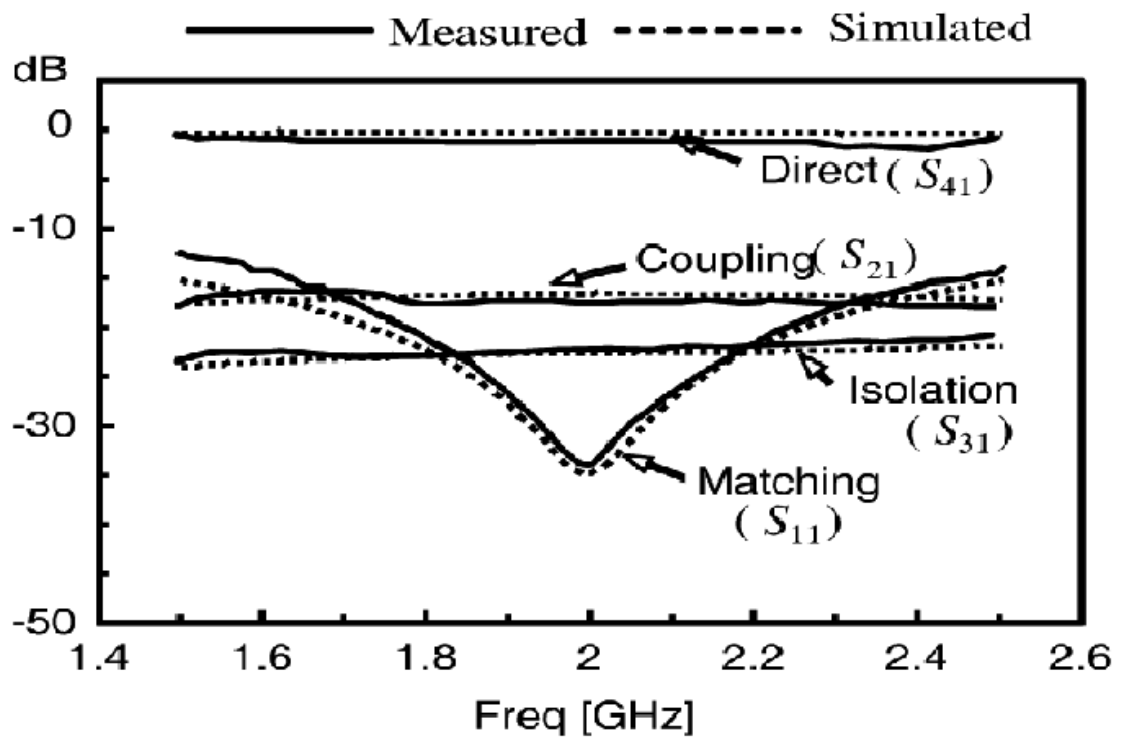


Figure 2.13: Measured results compared with simulation ones.

Based on the figure 2.13, the simulation result is good agreement with the measured.

2.4.3 Novel Trigonal Dual-mode Filter

The bandpass filter (BPF) is one of the most important components in microwave circuits. To meet the requirement of modern microwave communication systems, compact microwave BPFs with low insertion loss and high selectivity are in high demand. Dual-mode microstrip filters are attractive because each resonator can be used as a doubly tuned circuit, and therefore, the number of resonators required for a given degree of filter is reduced by half, resulting in a reduced-size filter structure. (Hong, J.-S., Lancaster, 2001).

In this paper, a novel design method for trigonal dual-mode filters with controllable transmission zeros is introduced. This filter consists of a trigonal open stub dual-mode resonator with cross-coupling between source and load. The technique of utilizing capacitive and inductive source-load coupling to improve the performance of this type of filter is explored intensively. Advantages of this type of filter include not only its dual-mode response, but also its controllable transmission zeros. Proposed bandpass filter are designed and fabricated to validate the design concept.

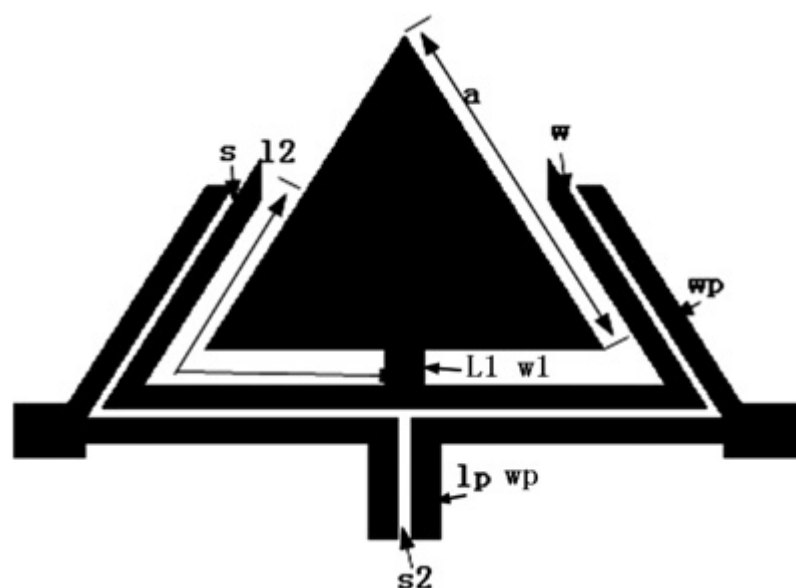


Figure 2.14: Layouts of the proposed trigonal dual-mode filter with capacitive S-L coupling.

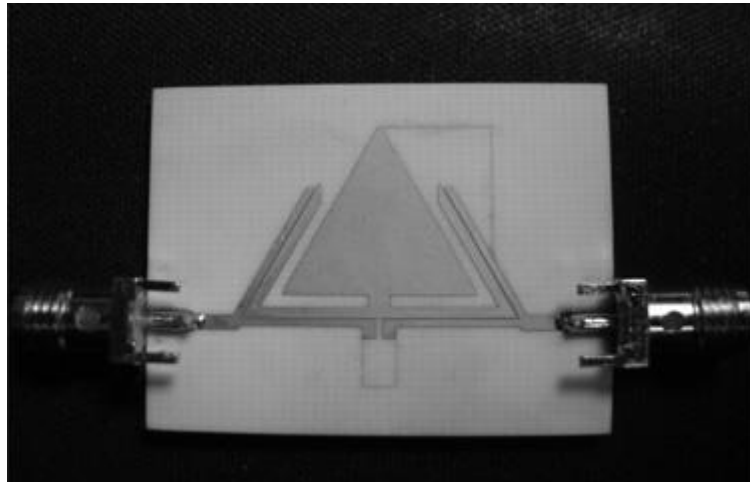


Figure 2.15: Prototype of trigonal dual-mode filter.

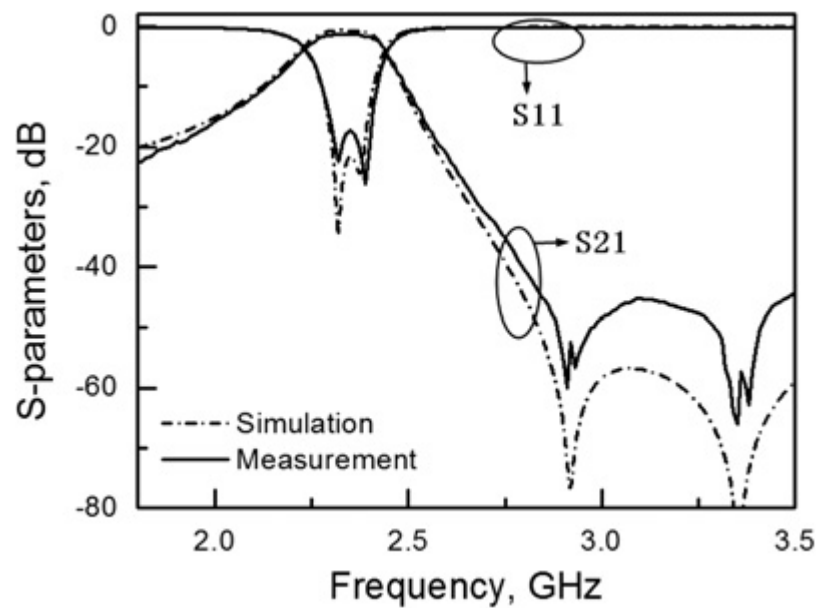


Figure 2.16: Simulated and measured frequency responses of the filter.

Figure 2.14 shows the layouts of the trigonal dual-mode filters. The filter consists of a trigonal open stub dual-mode resonator with cross-coupling between source and load. The proposed design filter is fabricated on the substrate Rogers RO4003, with a relative dielectric constant of 3.38 and thickness of 0.508mm. The prototype of trigonal dual-mode filters show in figure 2.15. Both measured and simulated results are plotted in Figure 2.16. According to the Figure 2.16, the 3dB bandwidth of the BPF is 0.25GHz at the centre frequency of 2.35GHz. Besides that,

two transmission zeros are realized at 2.90 and 3.35GHz. The insertion loss is less than 1dB from 2.3 to 2.45GHz, and the minimum insertion loss is 0.6dB.

2.4.4 Microstrip Band-pass Filter With Slotted Hexagonal Resonators and Capacitive Loading

As we know, modern mobile system has high requirements for bandpass filter (BPF) with many advantages such as smaller size, high selectivity, wide upper stop-band, low insertion loss and cost.

In this paper, a compact microstrip elliptic-function bandpass filter (BPF) is introduced. The techniques, etching slot and adding open stubs with capacitive loading, are applied to enhance the self-inductance and self-capacitance of the hexagonal open-loop resonators, which increases the electrical length of the resonator. Besides that, the capacitive coupling between two hexagonal resonators is enhanced too. So, the size is reduced and the insertion loss has been improved. (Wen Ming Li, Hai Wen Liu, Xiao Hua Li, Ahmed Boutejdar, Shu Xin Wang, Fu Tong, 2008).

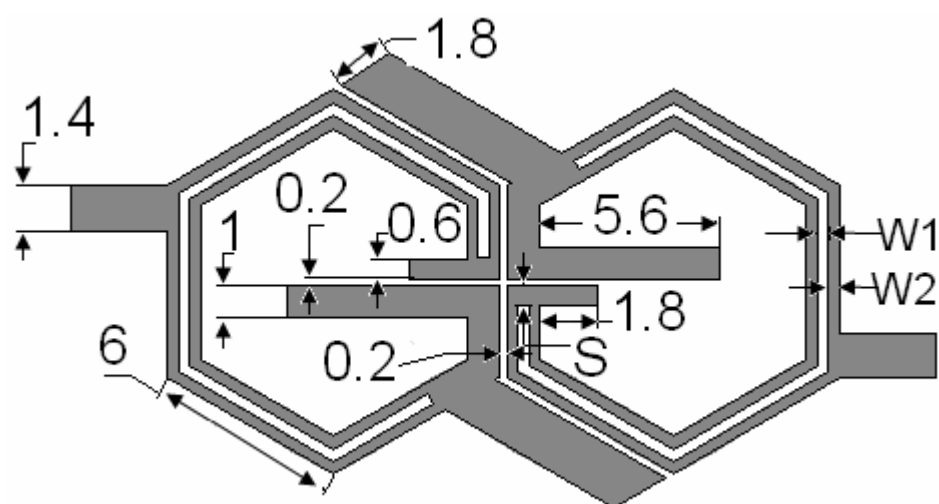


Figure 2.17: Layout of the hexagonal filters.

Figure 2.17 show the layout of the hexagonal. Extra transmission zeros maybe occurs when add one etching slot on each resonator. In addition, the extra transmission zero can be adjusted by changing the slot's length. Figure 2.18 is the prototype of the proposed filter which fabricated in FR-4 with 0.8mm of the thickness and dielectric constant of 4.5. The input and output line are chosen for the characteristics impedance of 50Ω microstrip lines.



Figure 2.18: Prototype of the proposed filter.

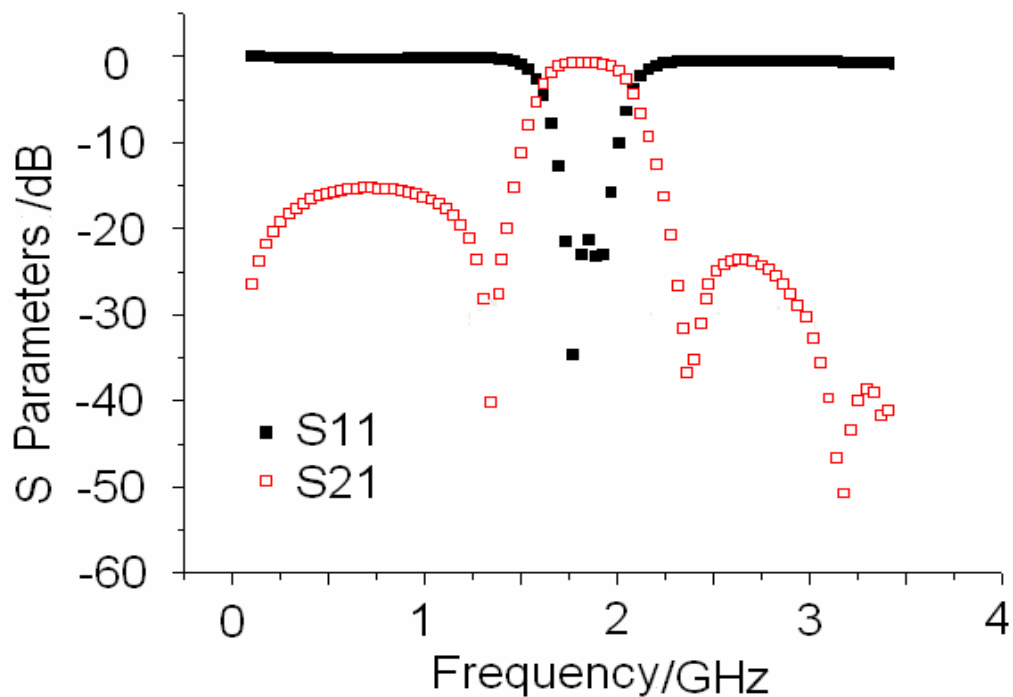


Figure 2.19: Measured results of the proposed filter.

Measured results of the proposed filter show in Figure 2.19, it verify that the proposed filter has a fraction bandwidth of 23% at centre frequency 1.84 GHz. Besides that, the filter has a return loss more than -15dB from 1.71 to 1.98 GHz. The insertion loss in the pass-band is less than -1.5dB. There are two transmission zeros on both sides of the pass-band which at 1.35 GHz and 2.37 GHz. Moreover, another transmission zero at 3.20GHz is -51dB. The results prove that, there is a good agreement between simulated and measured results.

2.5 Introduction of Simulation Tools

In order to carry out the experiments of this project, several tools and software were used. They include ANSOFT HFSS (High Frequency Structure Simulator), TxLine, CST Design Environment, Freelance Graphics, and so on. The following sections, background for HFSS will be introduced.

2.5.1 High Frequency Structure Simulator

High Frequency Structure Simulator (HFSS) is a registered trademark of Ansoft Corporation. HFSS is a high performance full wave electromagnetic (EM) filed simulator for arbitrary 3D volumetric passive device modelling that takes advantage of the familiar Microsoft Windows graphical user interface (GUI). It integrated simulation, visualization, solid modelling, and automation in an easy to learn environment and help to solve your 3D EM problems quickly and accurately.

Ansoft HFSS software has evolved over a period of year with the industries. It is the tool commonly used to development and virtual prototyping. With Ansoft HFSS, the scattering matrix parameters (S, Y, Z parameters) and also the visualization of the 3-D electromagnetic fields (near filed and far filed) can be done

easily. Besides that, it also can help to determine the signal quality, transmission path losses, and reflection coefficients.

2.5.2 TX-Line Calculator

TX-Line is free software; it is easy to use to analysis and synthesis of transmission line structures. TX-Line enables user to enter either physical characteristics or electrical characteristic for common transmission medium such as microstrip, stripline, coplanar waveguide, grounded coplanar waveguide, slotline and more.

CHAPTER 3

SLOT-BASED DIRECTIONAL COUPLER

3.1 Background

A slot-based directional coupler is a coupling device that can power division or power combining the signal. In Power division, an input signal is divided by coupler into two or more signal of lesser power. In this chapter, a slot-based directional coupler was analyzes. Moreover, simulations and measurements have been studied. Parametric analysis has been done to compare the result and discussed.

3.2 Configuration

Slot-based directional couplers have been successfully proposed and constructed in this research project. This proposed design was fabricated on the RT Duroid 5870 microstrip board (with a dielectric constants of $\epsilon_r = 2.33$ and thickness of the board = 1.57mm) by using photolithographic technique. It is a four-port directional coupler where Port 1 functions as an input port, Port 2 as a through port, Port 3 as a coupled port and Port 4 as an isolation port. The coupled line of the directional coupler is a slot line which construct at ground base.

Four of the microstrip transmission lines have the characteristic impedance of 50Ω . The proposed to designed these transmission lines have the characteristic impedance of 50Ω is because to control the impedance matching. The length of the coupled lines, l_1 increase when the single frequency of the device decreases. Two 90° bends are added to the coupled lines, the proposed is to reduce the size of the directional coupler. Input signal will pass through the transmission line and then pass down to the slot-based coupled line and transfer to through port and coupler port.

Figure 3.1 shows the top-down view of the proposed slot-based directional coupler. The blue colour is the slot-based coupled line of the directional coupler and the red colour is the microstrip transmission line. The detailed design parameters are given by: $l_1 = 60\text{mm}$, $l_2 = 18\text{mm}$, $w_1 = 4\text{mm}$, $w_2 = 4\text{mm}$, $w_3 = 3.5\text{mm}$, $g_1 = 6\text{mm}$, $g_2 = 13.1\text{mm}$, $g_3 = 12.1\text{mm}$, $g_4 = 16.6\text{mm}$, $g_5 = 12.1\text{mm}$, $d_1 = 4.5\text{mm}$, $d_2 = 4.5\text{mm}$, $d_3 = 4.5\text{mm}$ and $d_4 = 2.98\text{mm}$. The prototypes of the proposed slot-based directional coupler are shown in Figure 3.2 and Figure 3.3.

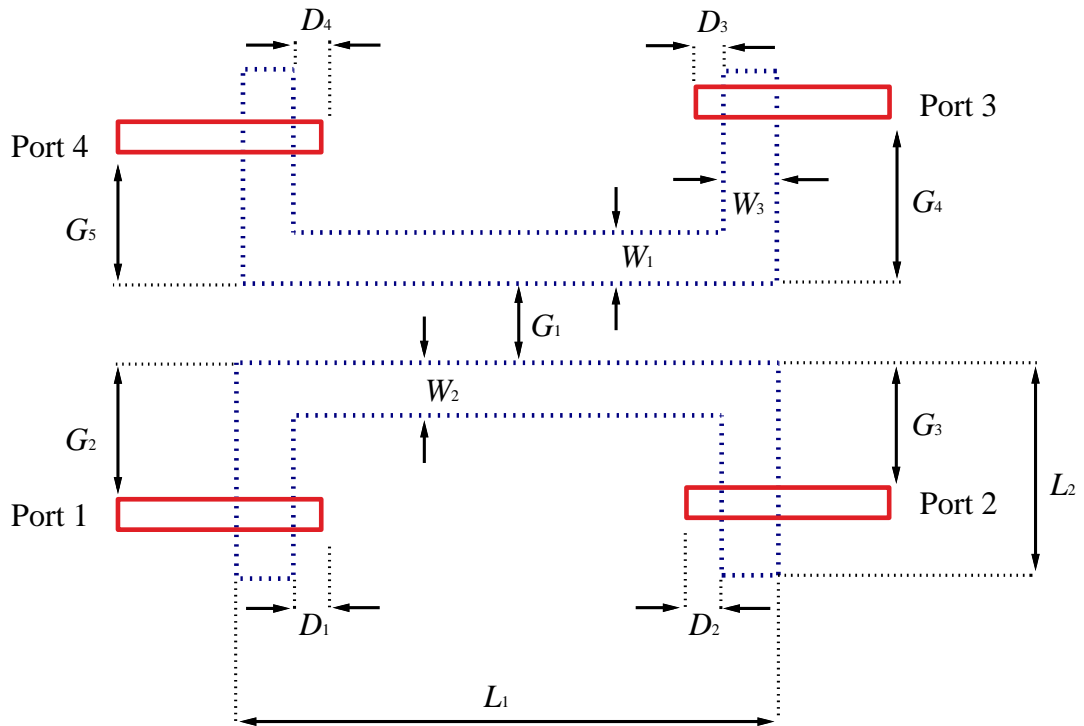


Figure 3.1: Configuration of the proposed microstrip slot-based directional coupler.

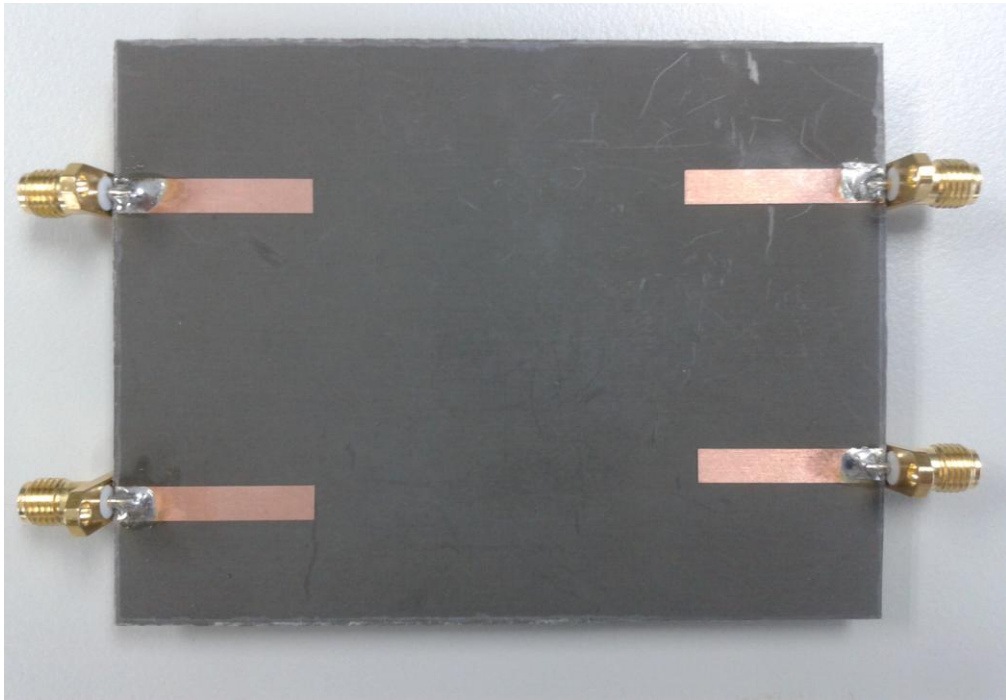


Figure 3.2: Prototype of the top view of the proposed slot-based directional coupler.

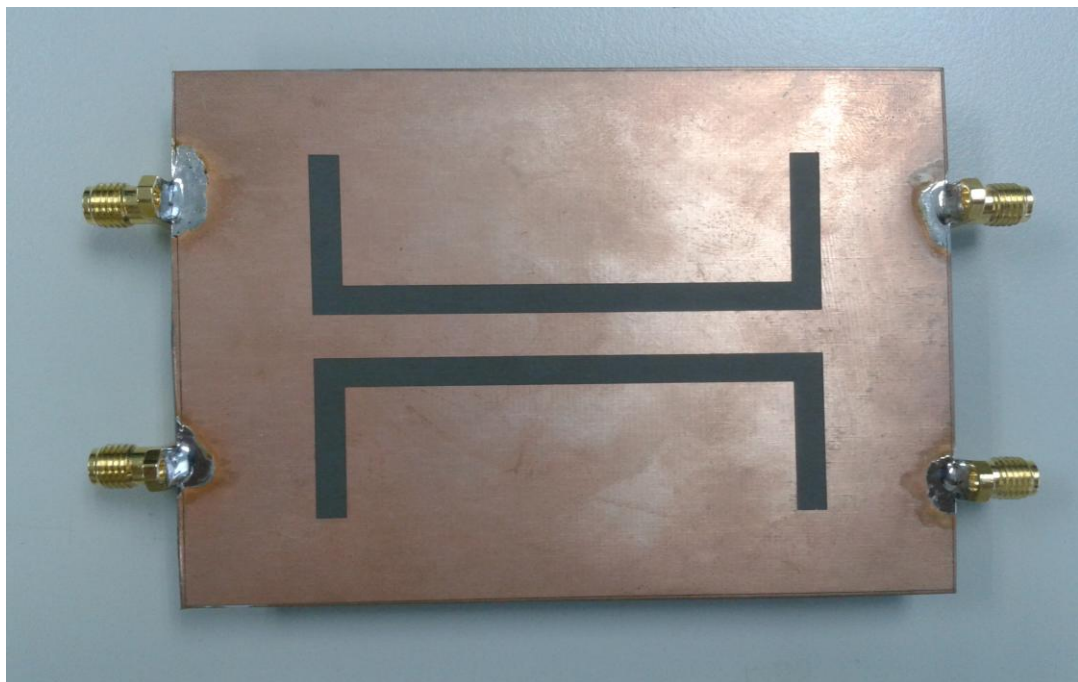


Figure 3.3: Prototype of the bottom view of the proposed slot-based directional coupler.

3.3 Simulation

The proposed slot-based directional coupler was simulated using Ansoft HFSS with all parameters given by: $l_1 = 60\text{mm}$, $l_2 = 18\text{mm}$, $w_1 = 4\text{mm}$, $w_2 = 4\text{mm}$, $w_3 = 3.5\text{mm}$, $g_1 = 6\text{mm}$, $g_2 = 13.1\text{mm}$, $g_3 = 12.1\text{mm}$, $g_4 = 16.6\text{mm}$, $g_5 = 12.1\text{mm}$, $d_1 = 4.5\text{mm}$, $d_2 = 4.5\text{mm}$, $d_3 = 4.5\text{mm}$ and $d_4 = 2.98\text{mm}$. Figure 3.4 shows the result of the simulation for the proposed slot-based directional coupler. The operating frequencies of the slot-based directional coupler are ranging from 2.77 GHz to 3.81 GHz with a total operating bandwidth of 1.04 GHz. The difference between the through port (S_{21}) and the coupled port (S_{31}) is $10\text{dB} \pm 1\text{dB}$. The signal of the input port need below -10dB and the signal of the isolation port need to below -15dB. Below is the calculation part for the center frequency and fractional bandwidth of the slot-based directional coupler:

Center Frequency

$$\begin{aligned}
 &= \frac{\text{LowerFrequency}, fL + \text{HighFrequency}, fH}{2} \\
 &= \frac{2.77\text{GHz} + 3.82\text{GHz}}{2} \\
 &= 3.30\text{GHz}
 \end{aligned}$$

Fractional Bandwidth

$$\begin{aligned}
 &= \frac{\text{HighFrequency}, fH - \text{LowerFrequency}, fL}{\text{CenterFrequency}, fC} \times 100\% \\
 &= \frac{3.82\text{GHz} - 2.77\text{GHz}}{3.30\text{GHz}} \times 100\% \\
 &= 31.82\%
 \end{aligned}$$

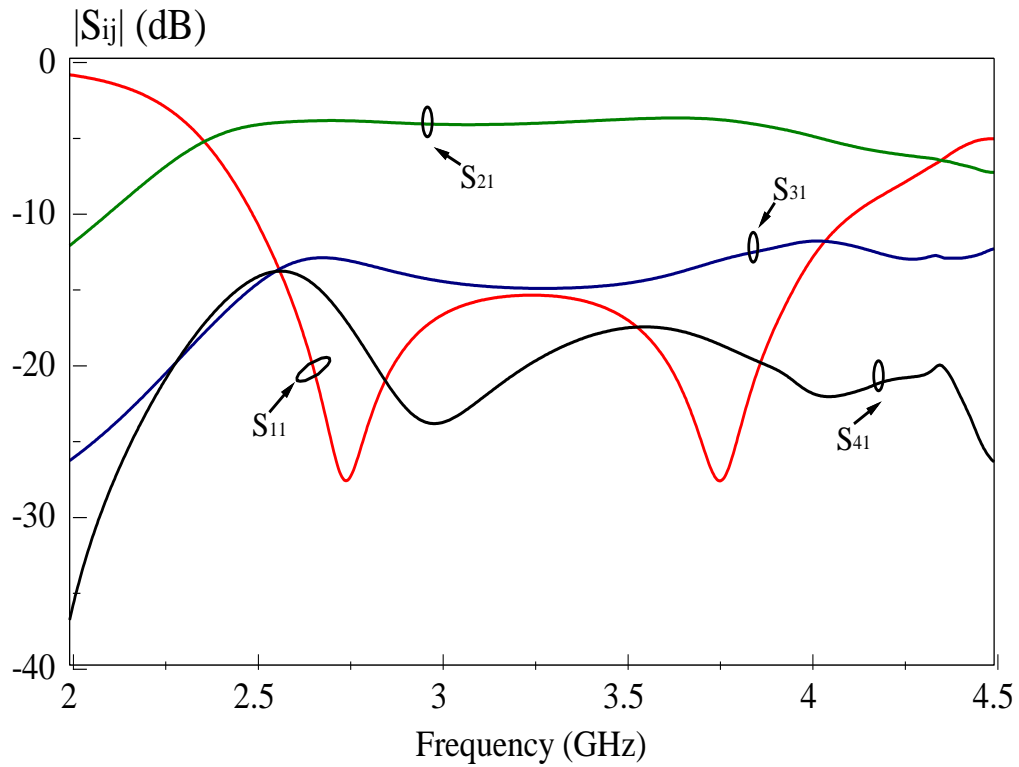


Figure 3.4: S-parameter of the proposed slot-based directional coupler.

3.4 Parametric Analysis

In order to obtain the optimal configuration of the proposed slot-based directional coupler, all the parameters were stepped up and stepped down few millimetres to analyze the effect of every parameter by using Ansoft HFSS software. All parameters will be discussed in detail, it include the gap between the coupled lines, length and width of the coupled lines, distance between the transmission lines with coupled line according to the configuration in figure3.1.

Analysis 1

- Parameter : l_1
- Optimum value : 60 mm
- Step-down value : 56 mm
- Step-up value : 64 mm

Results:

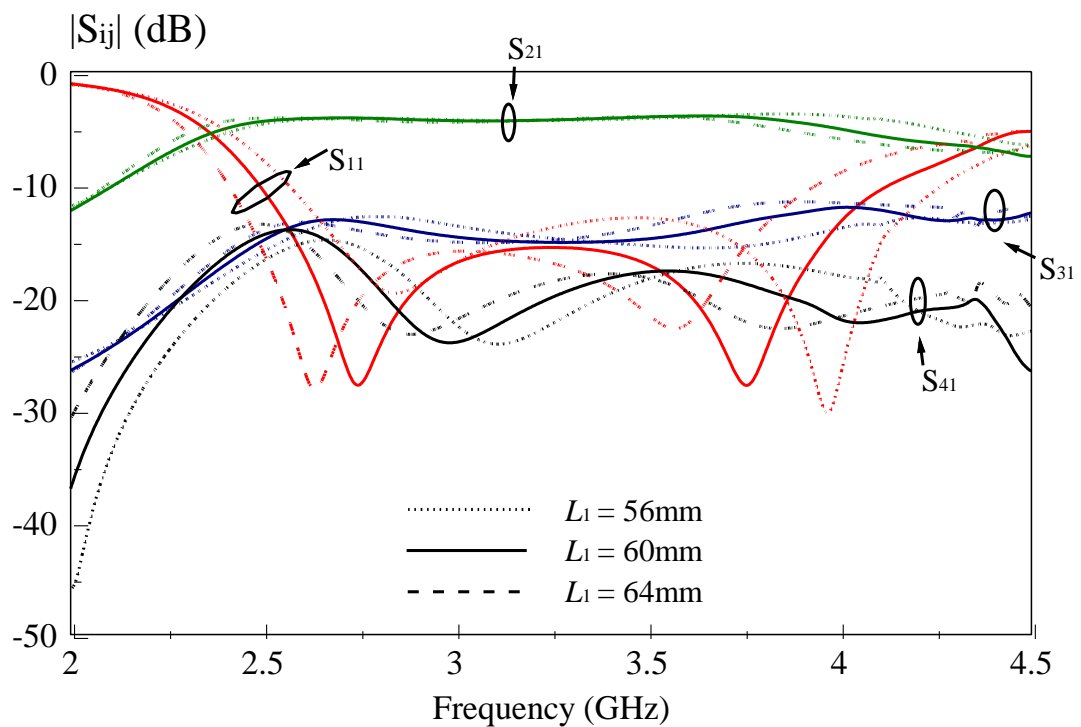


Figure 3.5: Effect of length l_1 on the slot-based directional coupler.

Description:

By changing the value of l_1 to 56mm, the operating frequencies are shift higher. It causes the operating bandwidth to reduce. When change the value of l_1 to 64mm, the operating frequencies is shift lower. In this figure show, when the length of coupled line increases, the operating frequency will decrease. Contrary the length of coupled line decrease, the operating frequency will increase.

Analysis 2

- Parameter : l_2
- Optimum value : 18 mm
- Step-down value : 17 mm
- Step-up value : 19 mm

Results:

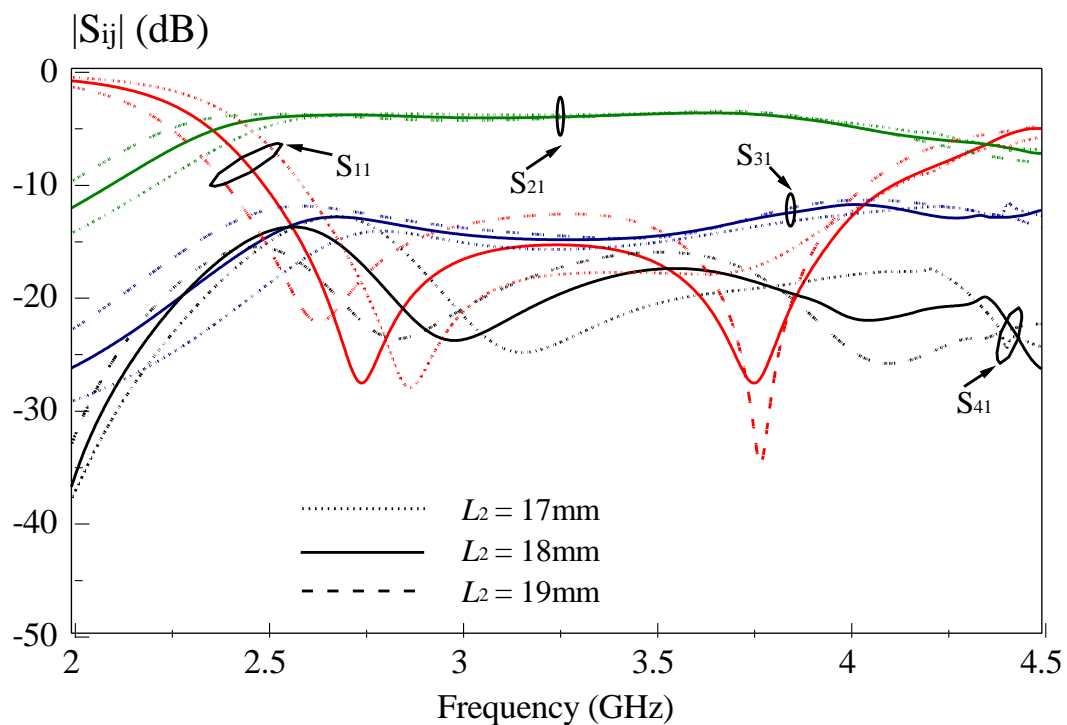


Figure 3.6: Effect of length l_2 on the slot-based directional coupler.

Description:

By varying the parameter l_2 , the operating frequencies are shifted. Besides that, S_{21} and S_{31} are slightly increase when the length of l_2 increase. It causes the operating bandwidth to reduce. When then length of l_2 decrease, the S_{21} and S_{31} are decrease. It causes the operating bandwidth decrease too. The optimal value of l_2 is more suitable, because it provide wide bandwidth and the S_{11} with a matching level below -10dB across the operating frequency.

Analysis 3

- Parameter : w_1 & w_2
- Optimum value : 4 mm
- Step-down value : 2 mm
- Step-up value : 6 mm

Results:

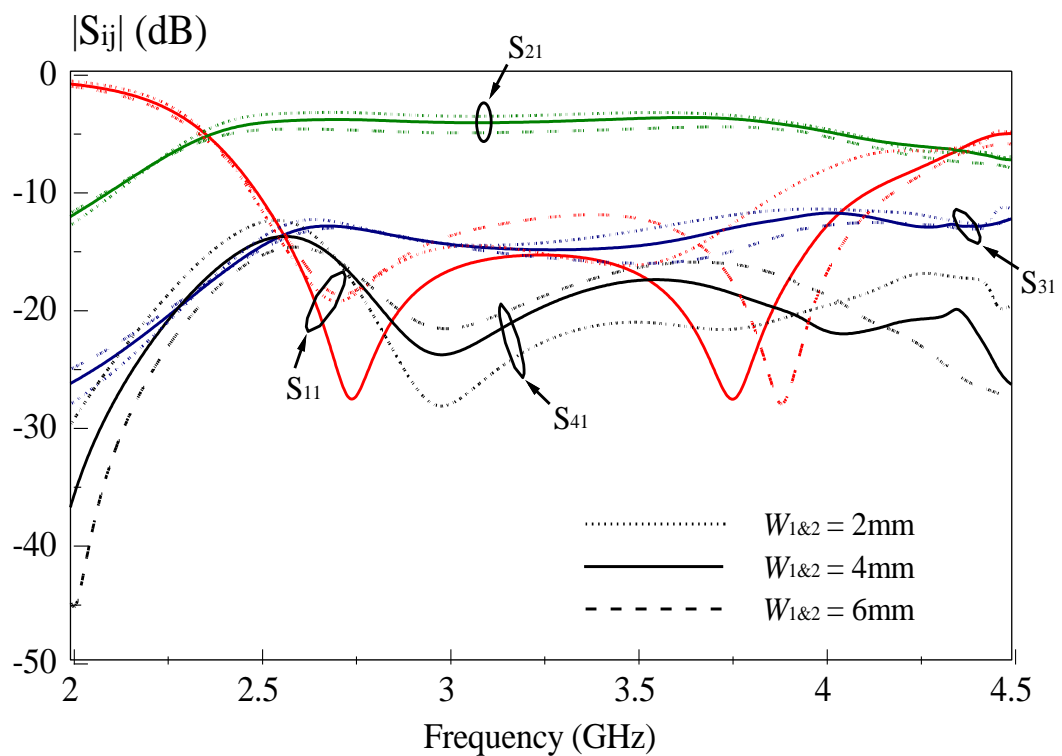


Figure 3.7: Effect of width w_1 & w_2 on the slot-based directional coupler.

Description:

The values of w_1 & w_2 have significant effect S_{11} on the proposed slot-based directional coupler. Moreover, these also cause the operating bandwidth to reduce as well. S_{31} will over the matching levels of the pole which is -15dB when the width w_1 & w_2 decrease.

Analysis 4

- Parameter : w_1
- Optimum value : 4 mm
- Step-down value : 2 mm
- Step-up value : 6 mm

Results:

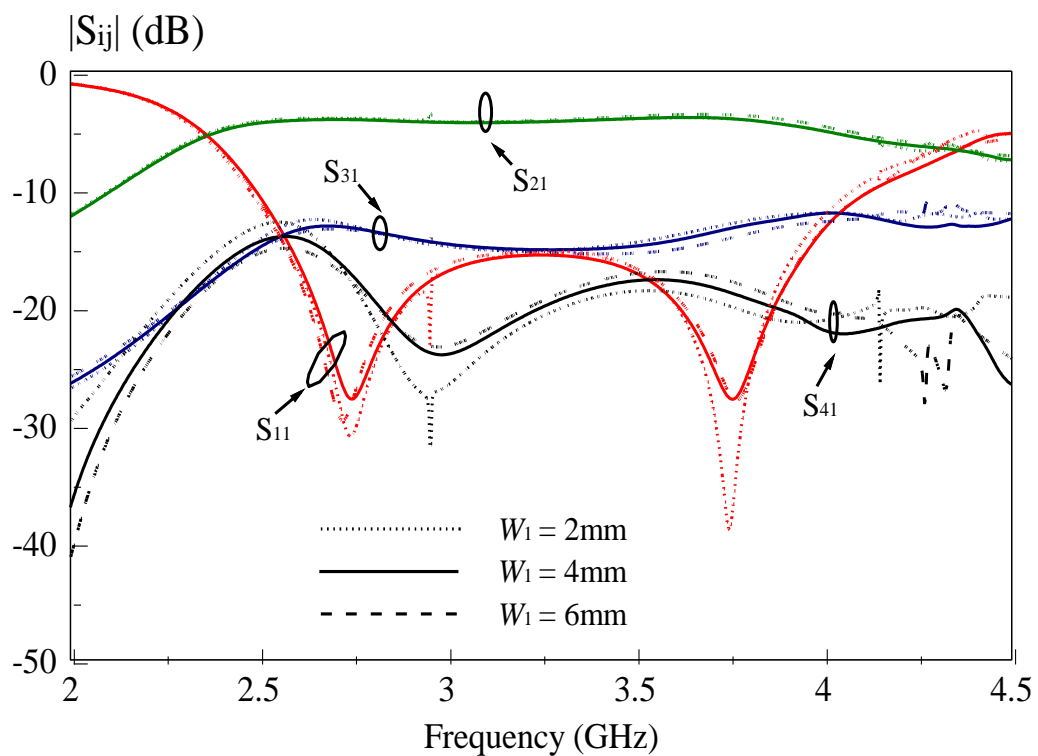


Figure 3.8: Effect of width w_1 on the slot-based directional coupler.

Description:

The parameter w_1 does not cause significant effect on the proposed slot-based directional coupler. It only affects the magnitude of the S_{11} . Besides that, S_{41} has increase a bit at the 2.5GHz, but it is out of ranging for the operating bandwidth. The optimal value of w_1 can give wide operating bandwidth compare to another two values.

Analysis 5

- Parameter : w_2
- Optimum value : 4 mm
- Step-down value : 2 mm
- Step-up value : 6 mm

Results:

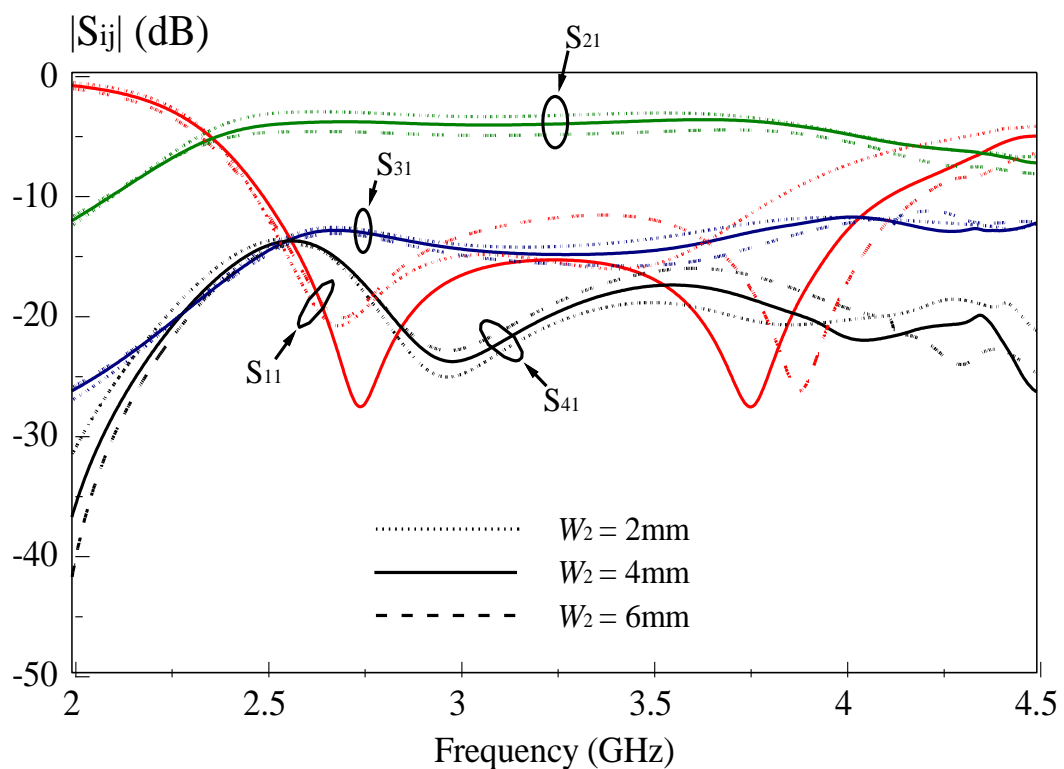


Figure 3.9: Effect of width w_2 on the slot-based directional coupler.

Description:

The w_2 value has effect on the reflection coefficient S_{11} . Furthermore, operating bandwidth is reduced too. According to Figure 3.9, width of w_2 stepped down, the S_{21} and S_{31} will be increase. Inverse, when the width of w_2 stepped up, the S_{21} and S_{31} will be decrease.

Analysis 6

- Parameter : w_3
- Optimum value : 3.5mm
- Step-down value : 1.5 mm
- Step-up value : 5.5 mm

Results:

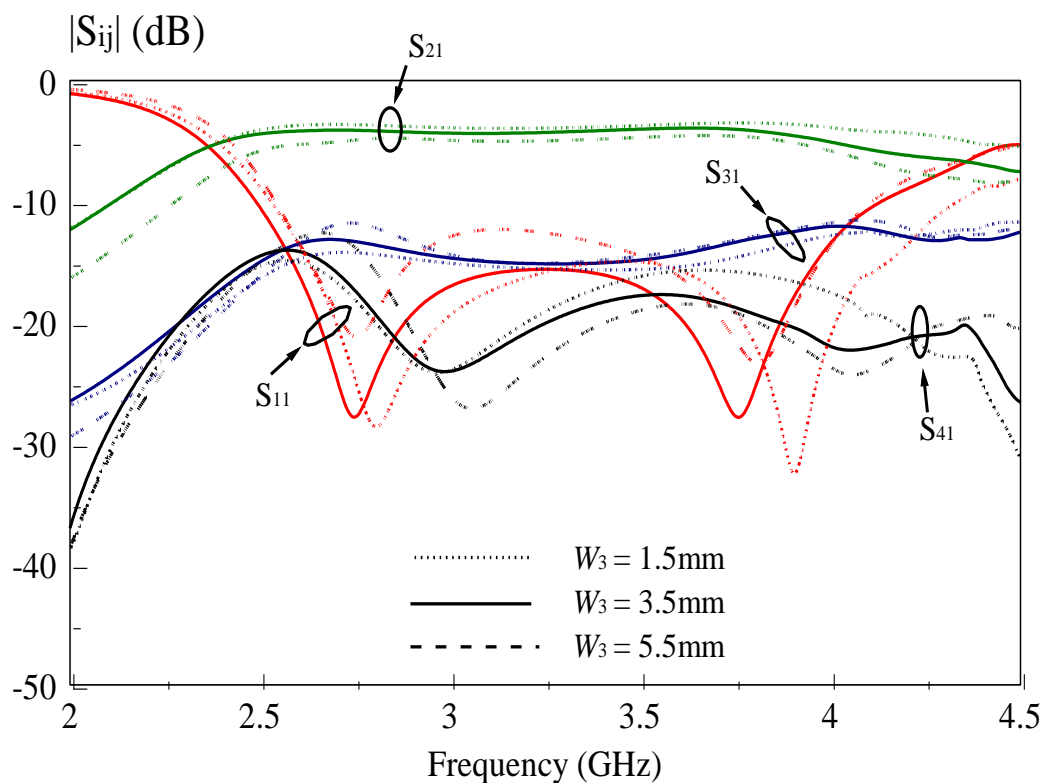


Figure 3.10: Effect of width w_3 on the slot-based directional coupler.

Description:

With reference to the amplitude response shown in Figure 3.10, we can clearly see that the width w_3 affects the coupling level of the proposed directional coupler. Besides that, it also shifts the curve of S_{11} when the width is altered. The optimum value of w_3 gives the best reflection coefficient S_{11} and wide operating bandwidth.

Analysis 7

- Parameter : g_1
- Optimum value : 6 mm
- Step-down value : 2 mm
- Step-up value : 12 mm

Results:

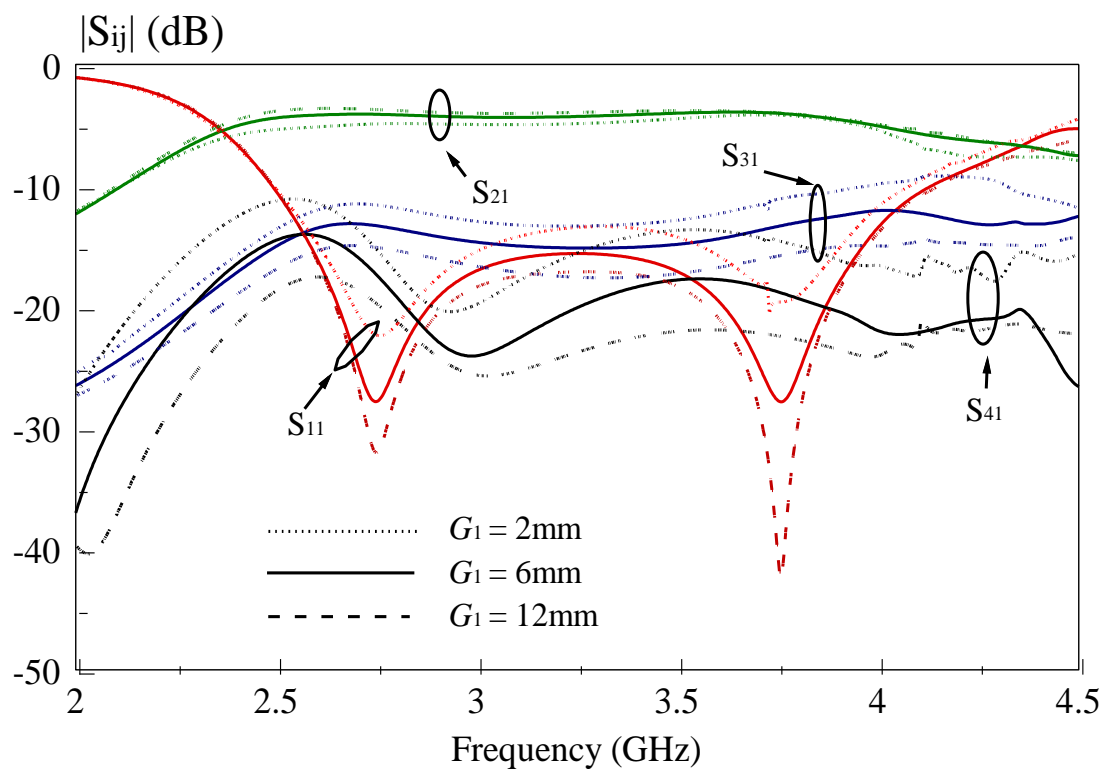


Figure 3.11: Effect of gap g_1 on the slot-based directional coupler.

Description:

Gap g_1 play an important role in the proposed directional coupler. Gap g_1 affect the coupling level between the through pole and coupled pole. When the parameter of g_1 stepped up, the coupling level will increase. Inverse, when the parameter of g_1 stepped down, the coupling level will decrease. In addition, the isolation level S_{41} will increase when the parameter of g_1 decrease and decrease when the parameter of g_1 increase.

Analysis 8

- Parameter : g_2
- Optimum value : 13.1 mm
- Step-down value : 12.1 mm
- Step-up value : 14.1 mm

Results:

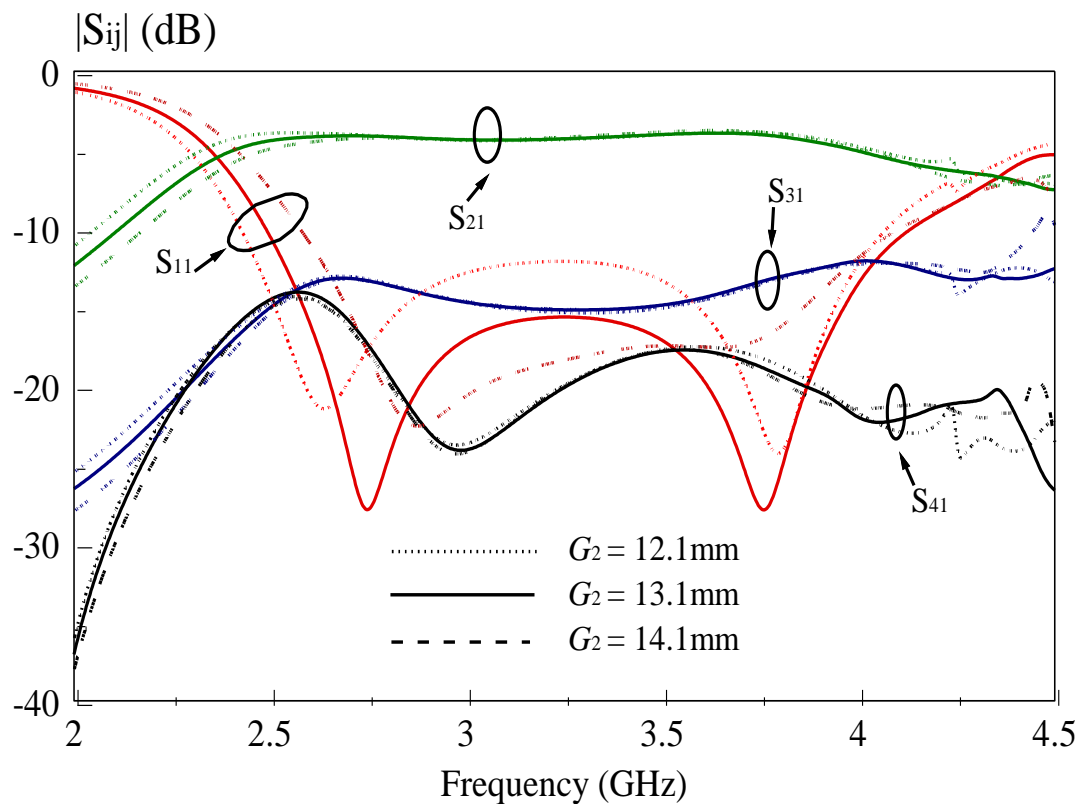


Figure 3.12: Effect of gap g_2 on the slot-based directional coupler.

Description:

Parameter g_2 does not bring much effect on the proposed directional coupler. It just shifts the curve of S_{11} when the gap size is altered. According to the Figure 3.12, the optimum value of g_2 gives best reflection coefficient S_{11} and wide operating bandwidth too.

Analysis 9

- Parameter : g_3
- Optimum value : 12.1 mm
- Step-down value : 11.1 mm
- Step-up value : 13.1 mm

Results:

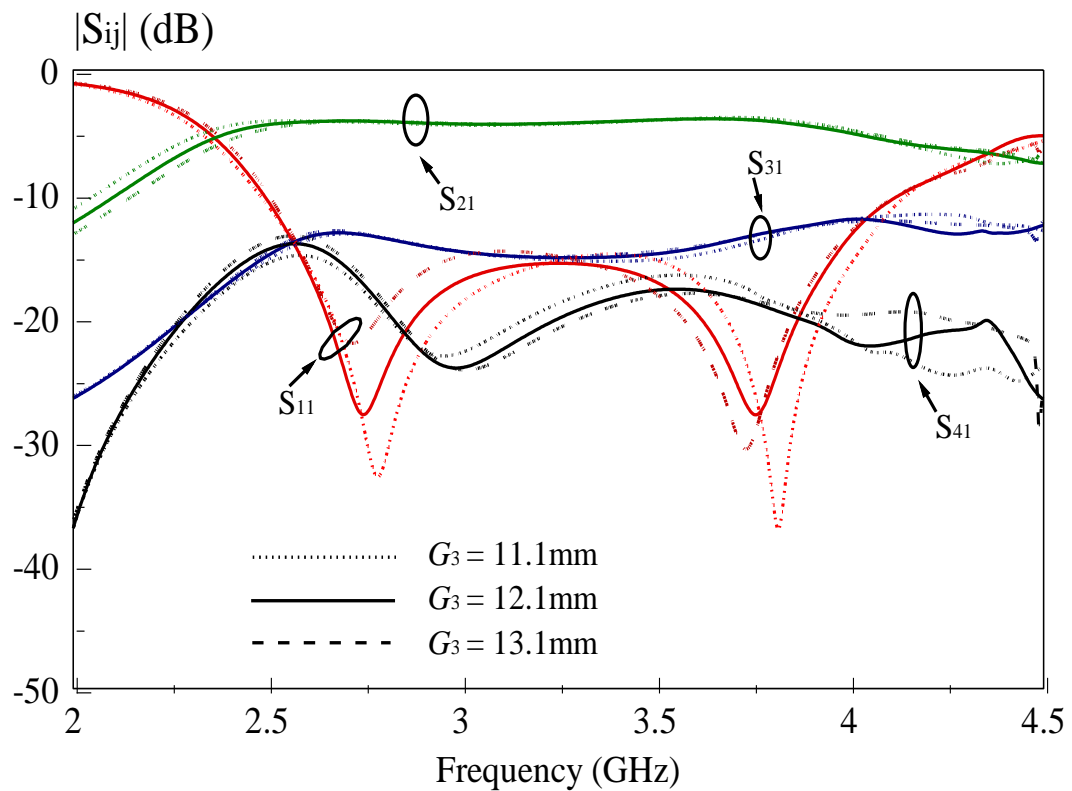


Figure 3.13: Effect of gap g_3 on the slot-based directional coupler.

Description:

In this project, the gap g_3 of the proposed directional coupler is designed to be 12.1 mm. By changing the value of g_3 , it has affected the isolation port. When the gap size is decrease, the curve of S_{41} has increase. When the gap size is increase, the curve of S_{41} has decrease. Besides that, the magnitude of the S_{11} will be changed when the gap size is altered. The curve of S_{21} has vary when the gap g_3 changed.

Analysis 10

- Parameter : g_4
- Optimum value : 16.6 mm
- Step-down value : 15.6 mm
- Step-up value : 17.6 mm

Results:

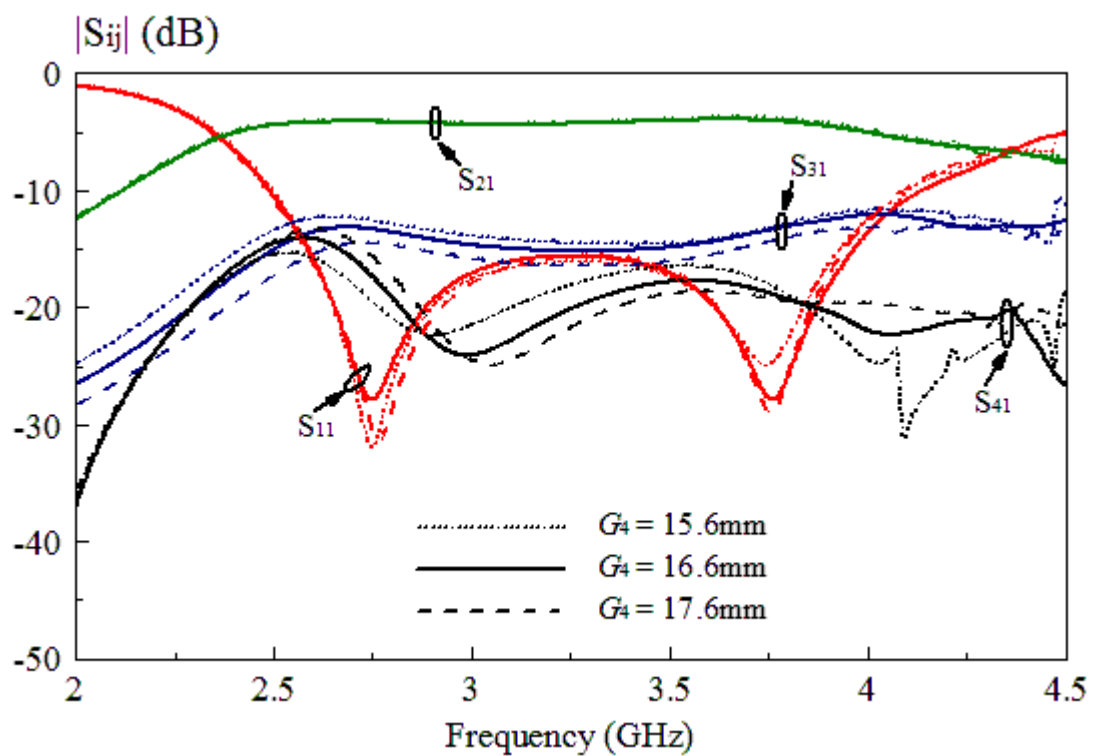


Figure 3.14: Effect of gap g_4 on the slot-based directional coupler.

Description:

The value of g_4 of the proposed directional coupler is designed to be 16.6mm. By changing the value of g_4 , the curve of S_{31} will vary. To obtain the coupling level within 10 ± 1 dB, the optimum value has provide good coupling level compare to other parameter.

Analysis 11

- Parameter : g_5
- Optimum value : 12.1 mm
- Step-down value : 11.1 mm
- Step-up value : 13.1 mm

Results:

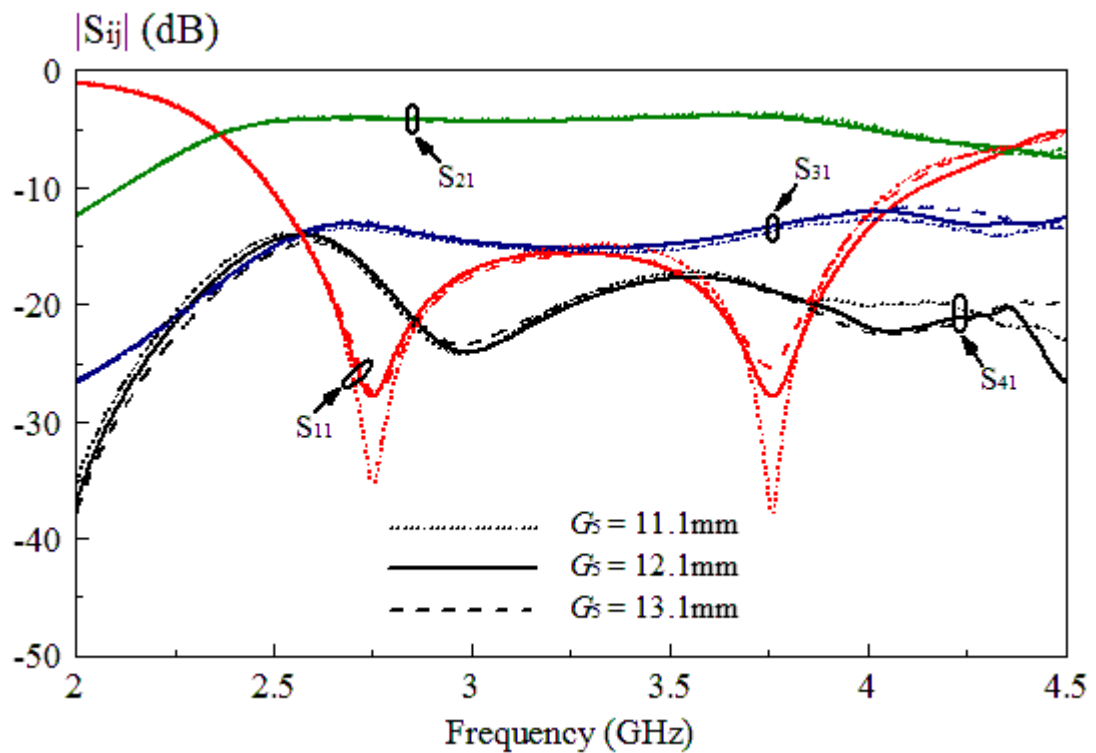


Figure 3.15: Effect of gap g_5 on the slot-based directional coupler.

Description:

The parameter g_5 does not cause significant effect on the proposed directional coupler. It only slightly affects the magnitude of the S_{11} of the proposed directional coupler. Besides that, when the parameter of g_5 has changing, the magnitude of S_{41} will vary too.

Analysis 12

- Parameter : d_1
- Optimum value : 4.5 mm
- Step-down value : 3.5 mm
- Step-up value : 5.5 mm

Results:

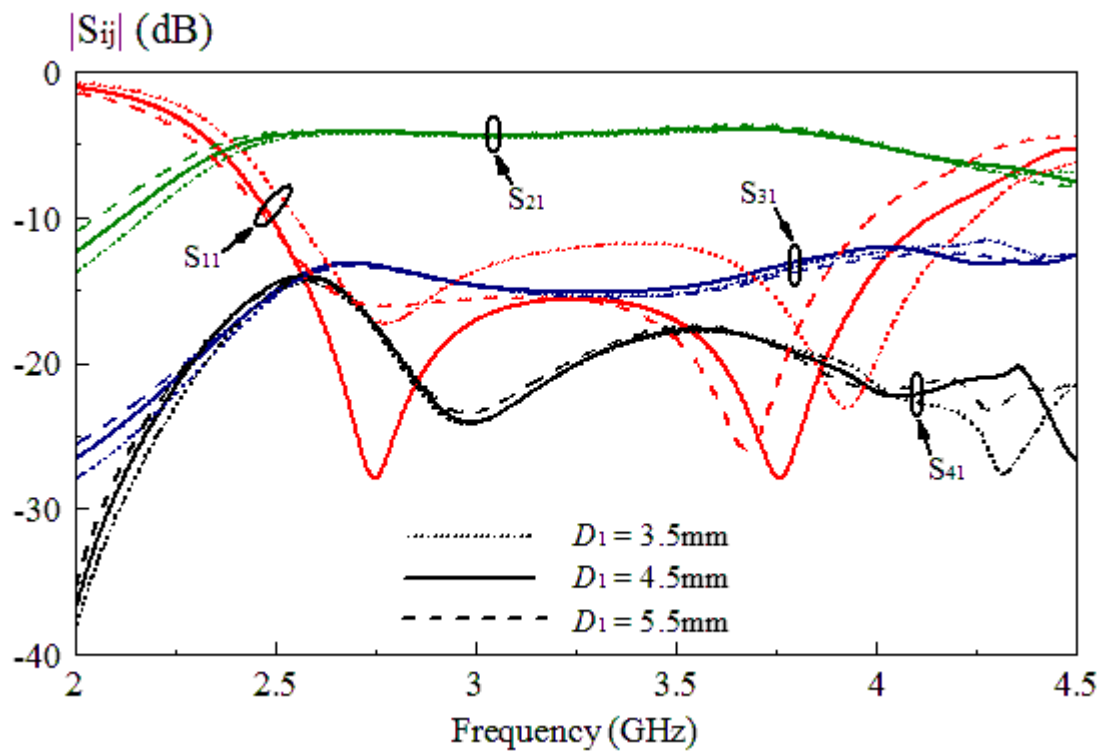


Figure 3.16: Effect of distance d_1 on the slot-based directional coupler.

Description:

By controlling the distance d_1 , the curve of S_{11} has shifted. The coupling level has slightly changed when the parameters of d_1 alter. The isolation level of the S_{41} is well maintained below -15dB in the ranging of the operating frequency.

Analysis 13

- Parameter : d_2
- Optimum value : 4.5 mm
- Step-down value : 3.5 mm
- Step-up value : 5.5 mm

Results:

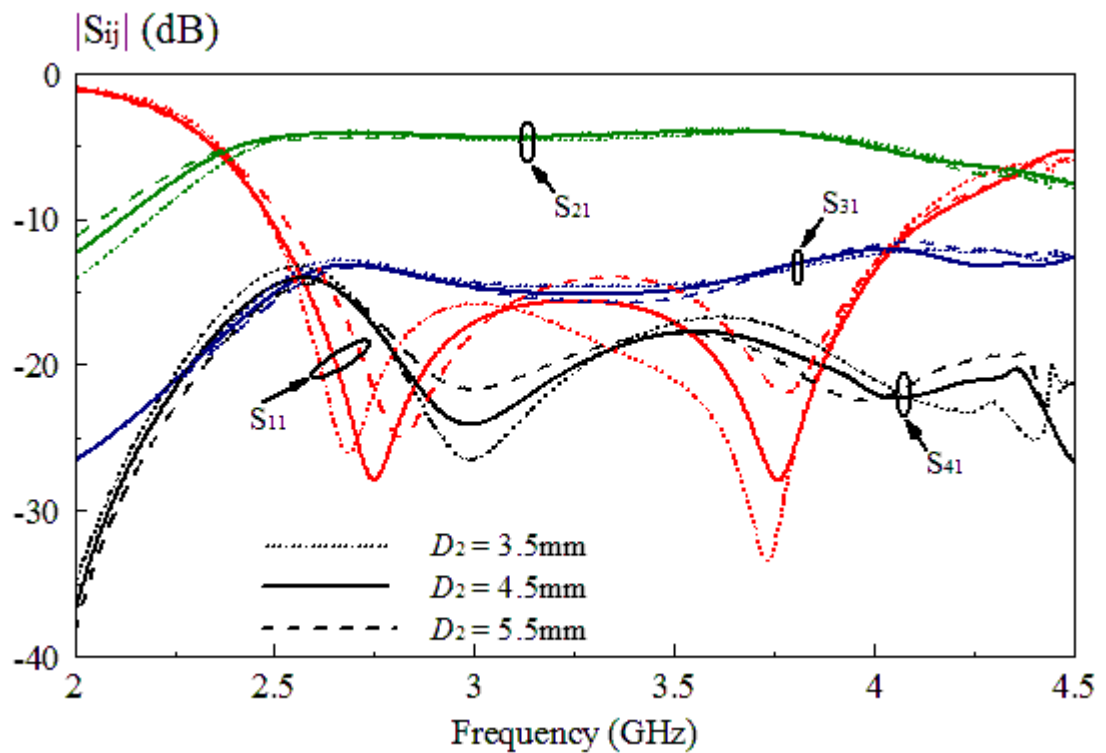


Figure 3.17: Effect of distance d_2 on the slot-based directional coupler.

Description:

The matching at Port 1 changes when the distance d_2 is altered. With reference to Figure 3.17, the matching level is maintained below -10dB even the distance d_2 is change. However, the position of the pole has change when the value d_2 is altered. Besides that, S_{21} and S_{31} are slightly altered when the value of d_2 is changing.

Analysis 14

- Parameter : d_3
- Optimum value : 4.5 mm
- Step-down value : 2.5 mm
- Step-up value : 6.5 mm

Results:

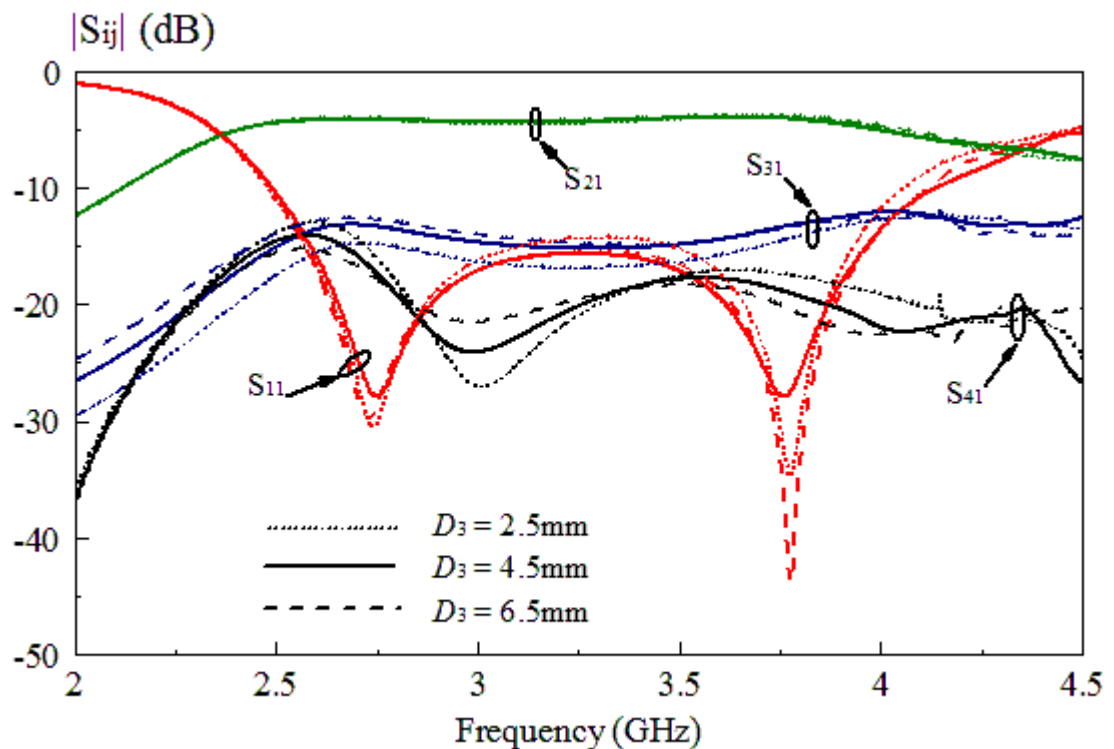


Figure 3.18: Effect of distance d_3 on the slot-based directional coupler.

Description:

By controlling the parameter d_3 , the coupling level of the proposed directional coupler can be adjusted. When the distance d_3 is 2.5mm, the coupling level of the proposed directional coupler has change smaller. When the distance d_3 is 6.5mm, the coupling level has increase large. Besides that, the magnitudes of S_{11} and S_{41} have slightly changed when the parameter d_3 is altered. As a result, the optimum value of d_3 provide the most wide operating bandwidth (within 10dB \pm 1dB).

Analysis 15

- Parameter : d_4
- Optimum value : 2.98 mm
- Step-down value : 0.98 mm
- Step-up value : 4.98 mm

Results:

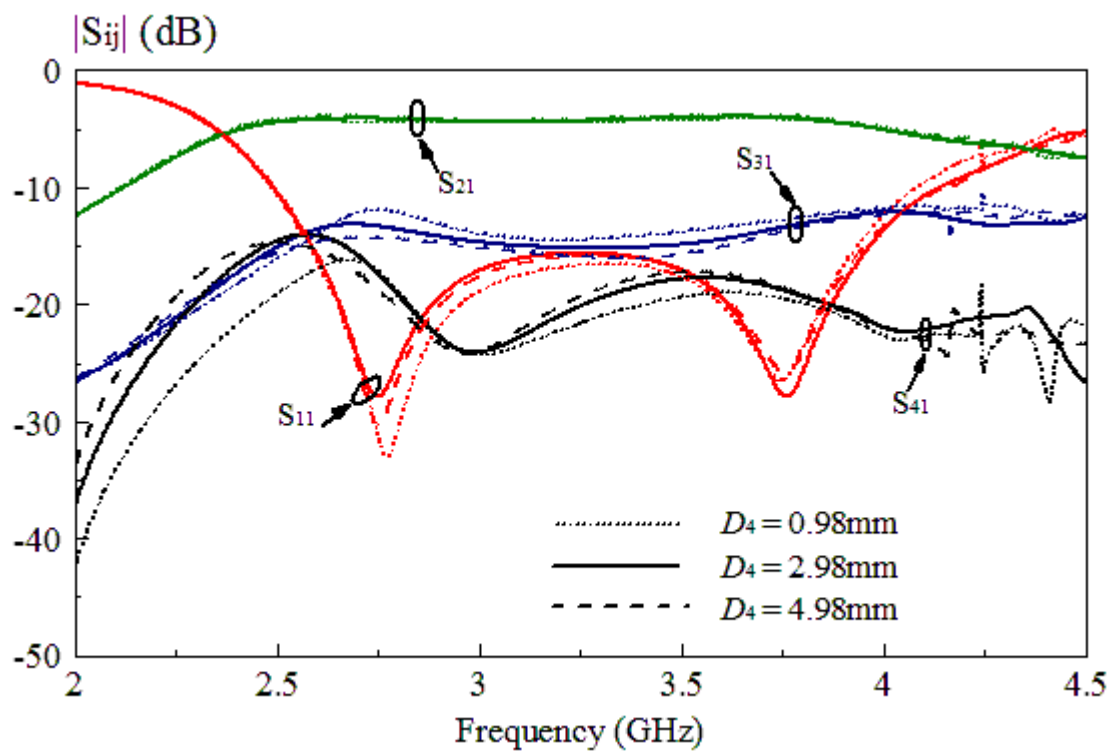


Figure 3.19: Effect of distance d_4 on the slot-based directional coupler.

Description:

Figure 3.19 shows the effect of d_4 on the amplitude response. It can be seen that the coupling level will be altered if the value of d_4 changes. Apart from that, the curve of S_{41} has a slight change when the parameter of d_4 varies. Moreover, the magnitude of S_{11} will slightly decrease when the value of d_4 changes.

3.5 Results

The proposed configuration of the slot-based directional coupler was simulated by using Ansoft HFSS software. After get the best simulation result, the proposed slot-based directional coupler was fabricated using photolithographic process. In order to examine the performances of the slot-based directional coupler, measurements were carried out by using the Rohde & Schwarz ZVB8 Vector Network Analyzer (VNA). Each ports amplitude responses of the proposed slot-based directional coupler were carried out. Comparison has made to compare the simulation result with the experiment measured result. Figure 3.20 show the simulated and measured amplitude responses of the slot-based directional coupler.

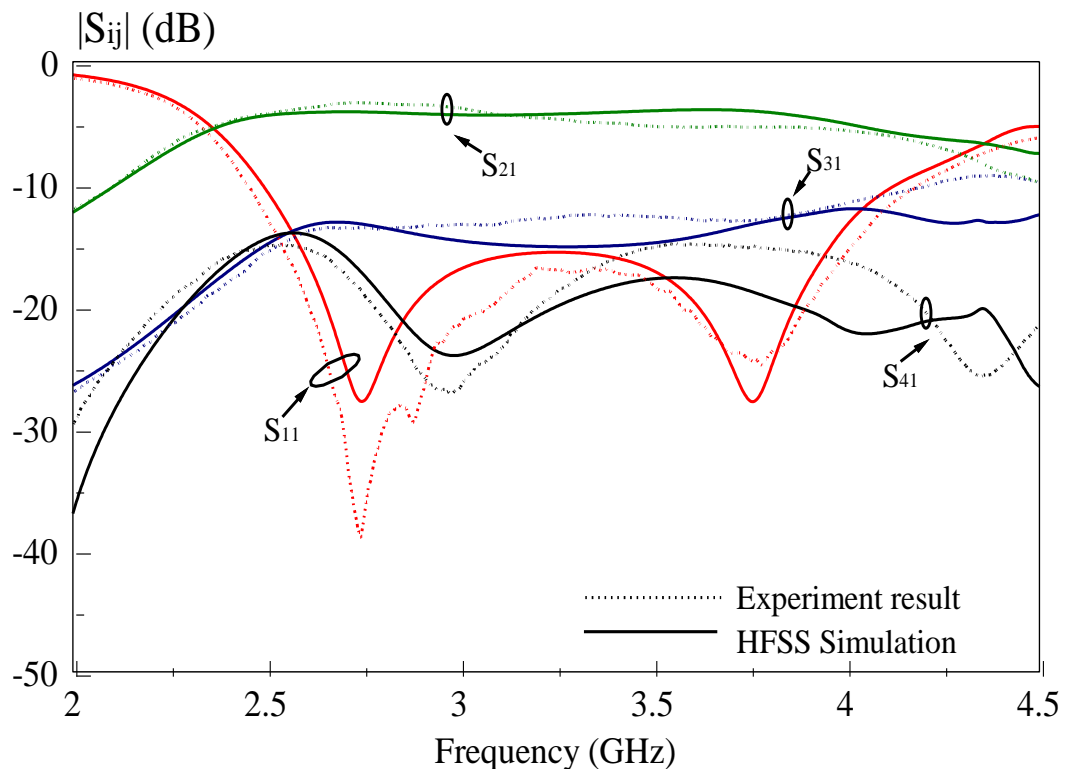


Figure 3.20: Simulated and measured amplitude responses of the slot-based directional coupler.

Based on the results above, it is obvious that a slot-based directional coupler can be realised with the proposed design. According to the Figure 3.20, the S_{21} of the experimental result has decrease between 3GHz to 4.5 GHz .Besides that, the S_{31} of

the experimental result has increase between 2.75GHz to 3.75GHz. These make the operating bandwidth reduced. Based on the results, the operating frequency of the experimental result is from 2.53 GHz to 3.10 GHz which the total bandwidth of 0.57GHz. It is 63.64% of the HFSS simulation result. From the figure 3.20, even the curve of S_{11} and S_{41} is vary, but it are still in the matching level which are -10dB for S_{11} and -15dB for S_{41} . So, this does not cause any significant effect to the proposed slot-based directional coupler. Table 3.1 show the comparison of the experiment and HFSS simulation results.

Table 3.1: Comparison of the experiment and HFSS simulation results

	Experiment	HFSS Simulation
f_L (GHz) / f_H (GHz)	2.53 / 3.10	2.77 / 3.82
f_c (GHz)	2.82	3.30
Fractional Bandwidth (%)	20.25	31.82

3.6 Discussion

The function of the slot-based directional coupler is same to conventional directional coupler. The proposed slot-based directional coupler is used to power combining or power division. The proposed slot-based directional coupler send the signal to the input port, S_{11} then divide the signal and send to the through port, S_{21} and coupler port, S_{31} but no to isolation port, S_{41} . The power for the signal has become lower compare to the initial signal. The signal through to input port will has reflection, known as reflection loss. Besides that, the signal transfer from the input port to the direct and coupler port will get insertion loss. To obtain a best result, the reflection loss and insertion loss should have to control and minimize it.

According to table 3.1, the experimental result is poor compare to simulation result which only 20.25% compare to 31.82%. The problems are the direct and coupled signals vary with frequency and make the coupling level reduce. It may be

because of the distance of d_3 and d_4 have changed during the etching process, known as over etching. Based on the parametric analysis in Section 3.4, several parameters are found which can affect the coupling level. Parameter such as w_2 , w_3 , g_1 , g_4 , d_3 and d_4 are crucial for the determination of the coupling level for the slot-based directional coupler. Parameters like l_1 , l_2 , g_2 and d_1 are the important factor for the operating frequency. By knowing the characteristics and effects of all the design parameters, the proposed slot-based directional coupler can be easily optimized. The reason author did not re-construct the proposed directional coupler is because the time is limited which not allow the author to re-construct it.

During the measurement process by using the Rohde & Schwarz ZVB8 Vector Network Analyzer (VNA), some of the process needs to be careful because it can affect the accuracy of the result. Before using Vector Network Analyzer to measure the circuit board, calibration process should be done properly. It ensure the VNA and the connector did not any reflection loss. Apart from that, Rohde & Schwarz ZVB8 Vector Network Analyzer only can measure single port which means it has only 1 input and 1 output. So, author can only measure the amplitude response one by one. Another two port without to measure need to mount the 50Ω match. It to ensure these ports is matching with the transmission line.

CHAPTER 4

SLOT-BASED BANDPASS FILTER

4.1 Background

A slot-based bandpass filter is a device that can filter the signal which allows the certain range frequencies to pass and rejects frequencies outside that range. The range between the lower and upper -3dB cut-off points being known as the bandwidth of the filter. In this chapter, a slot-based bandpass filter was analyzed. Simulations and parametric analysis has been done. Based on the information, discussion of the slot-based bandpass filter has been made.

4.2 Configuration

A slot-based bandpass filter that operates across the passband with a center frequency of 1.235GHz was designed. Substrate FR-4 (with dielectric constants of $\epsilon_r = 4.4$ and thickness of the board = 1.57mm) was used in this project. The input and output port of the proposed filter are designed with the characteristic impedance of 50 Ω microstrip lines. The proposed filter used the slot-based technique to transmit the signal.

The proposed slot-based bandpass filter was simulated using the Ansoft HFSS software. Figure 4.1 shows the top down view of the proposed slot-based bandpass filter. The blue colour structure of the Figure 4.1 is slot which construct in the ground based. The red colour structure is the microstrip transmission line for proposed bandpass filter. The detailed designed parameters are given by: $g_1 = 5\text{mm}$, $g_2 = 3\text{mm}$, $g_3 = 3\text{mm}$, $g_4 = 1\text{mm}$, $g_5 = 1\text{mm}$, $w_1 = 3.5\text{mm}$, $w_2 = 0.5\text{mm}$, $w_3 = 0.5\text{mm}$, $d_1 = 15.575\text{mm}$, $d_2 = 13.075\text{mm}$, $l_1 = 15\text{mm}$, $l_2 = 20\text{mm}$, $l_3 = 25\text{mm}$, $l_4 = 30\text{mm}$, $l_5 = 25\text{mm}$, $l_6 = 32\text{mm}$, $l_7 = 15\text{mm}$, $l_8 = 20\text{mm}$, $l_9 = 26\text{mm}$ and $l_{10} = 26\text{mm}$.

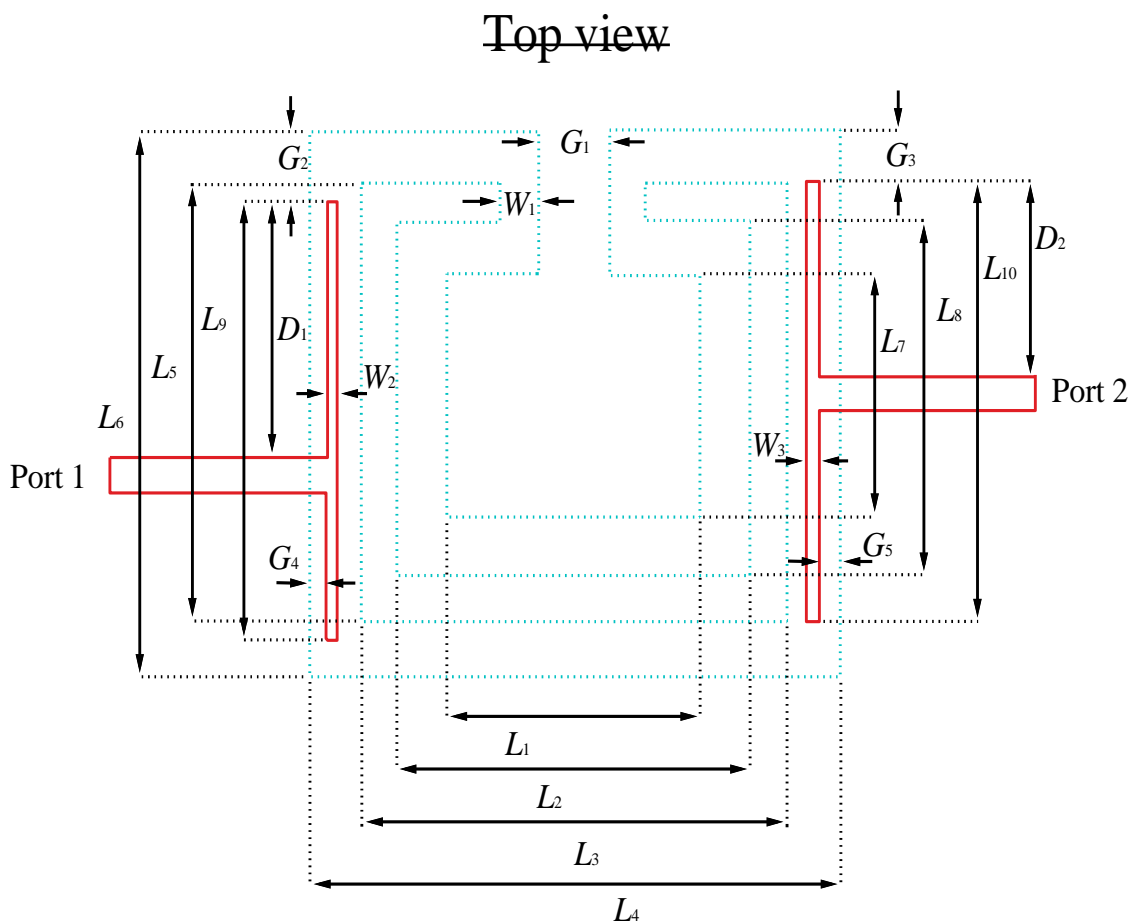


Figure 4.1: Top-down view of the proposed slot-based bandpass filter.

4.3 Simulation

The proposed slot-based bandpass filter was simulated using Ansoft HFSS with all parameters given by: $g_1 = 5\text{mm}$, $g_2 = 3\text{mm}$, $g_3 = 3\text{mm}$, $g_4 = 1\text{mm}$, $g_5 = 1\text{mm}$, $w_1 = 3.5\text{mm}$, $w_2 = 0.5\text{mm}$, $w_3 = 0.5\text{mm}$, $d_1 = 15.575\text{mm}$, $d_2 = 13.075\text{mm}$, $l_1 = 15\text{mm}$, $l_2 = 20\text{mm}$, $l_3 = 25\text{mm}$, $l_4 = 30\text{mm}$, $l_5 = 25\text{mm}$, $l_6 = 32\text{mm}$, $l_7 = 15\text{mm}$, $l_8 = 20\text{mm}$, $l_9 = 26\text{mm}$ and $l_{10} = 26\text{mm}$. Figure 4.2 shows the result of the simulation for the proposed slot-based bandpass filter. According to the Figure 4.2, the 3dB bandwidth of the BPF is 0.13GHz which from 1.17 to 1.30GHz and center frequency of 1.235 GHz. Besides that, the filter has a return loss more than -13dB from 1.21 to 1.29 GHz. The insertion loss in the passband is less than 2.77dB. The minimum insertion loss in the passband is only 0.5dB. Furthermore, there has one transmission zero at 1.69 GHz which is -42dB. Below is the calculation part for the center frequency and fractional bandwidth of the slot-based bandpass filter:

Center Frequency

$$\begin{aligned}
 &= \frac{\text{LowerFrequency, } fL + \text{HighFrequency, } fH}{2} \\
 &= \frac{1.17\text{GHz} + 1.30\text{GHz}}{2} \\
 &= 1.235\text{GHz}
 \end{aligned}$$

Fractional Bandwidth

$$\begin{aligned}
 &= \frac{\text{HighFrequency, } fH - \text{LowerFrequency, } fL}{\text{CenterFrequency, } fC} \times 100\% \\
 &= \frac{1.30\text{GHz} - 1.17\text{GHz}}{1.235\text{GHz}} \times 100\% \\
 &= 10.53\%
 \end{aligned}$$

The calculation in above shows the proposed bandpass filters has a fractional bandwidth of 10.53% at center frequency 1.235GHz.

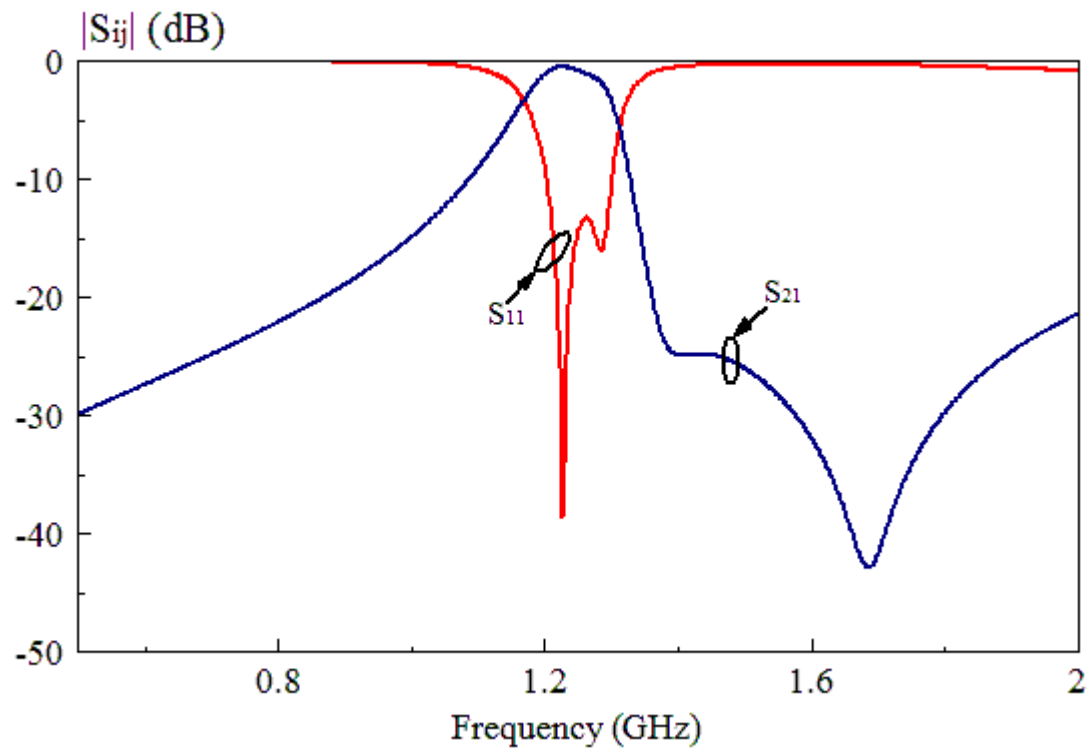


Figure 4.2: Simulated result of the proposed slot-based bandpass filter.

4.4 Parametric Analysis

In order to obtain the optimal configuration of the proposed slot-based bandpass filter, all the design parameters were analyzed using Ansoft HFSS to study the effects. In following section, all parameters will be discussed in detail in here.

Analysis 1

- Parameter : g_1
- Optimum value : 5 mm
- Step-down value : 4 mm
- Step-up value : 6 mm

Results:

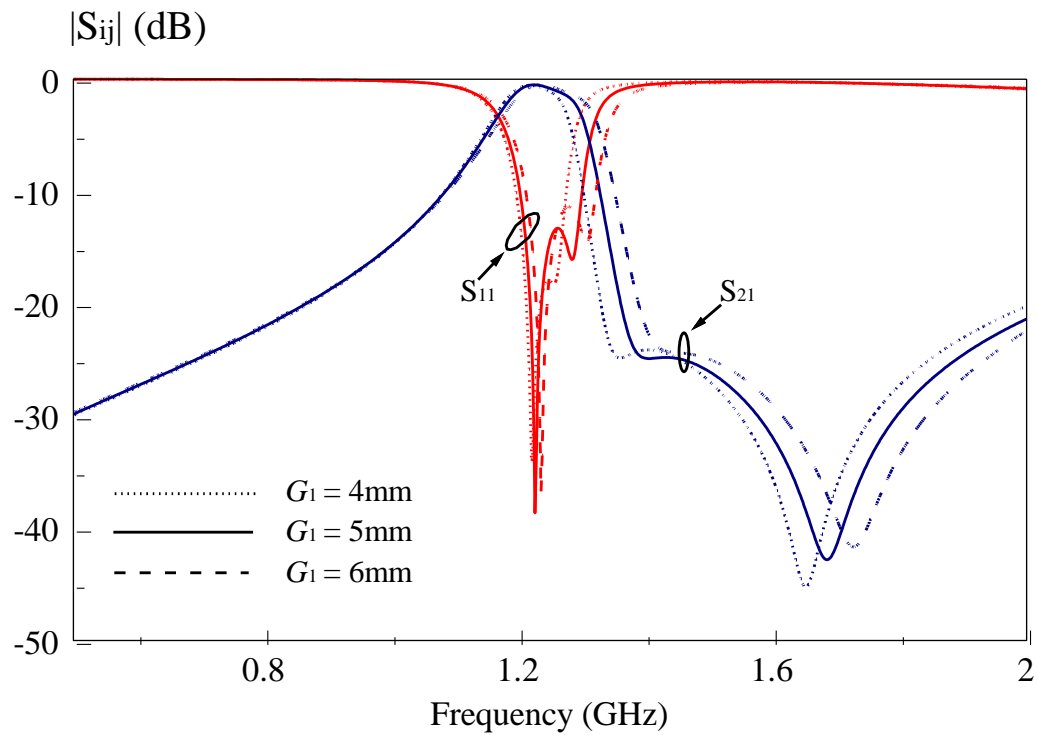


Figure 4.3: Effects of gap g_1 on the slot-based bandpass filter.

Description:

By changing the value of g_1 to 4mm, bandwidth of the BPF has reduced. Besides that, the curve of S_{11} has been change as well. When the value of g_1 changed to 6mm, bandwidth of the BPF has increased. However, the BPF has a return loss more than -13dB from 1.29 to 1.31GHz, which become smaller compared to optimum value 5mm.

Analysis 2

- Parameter : g_2
- Optimum value : 3 mm
- Step-down value : 2 mm
- Step-up value : 4 mm

Results:

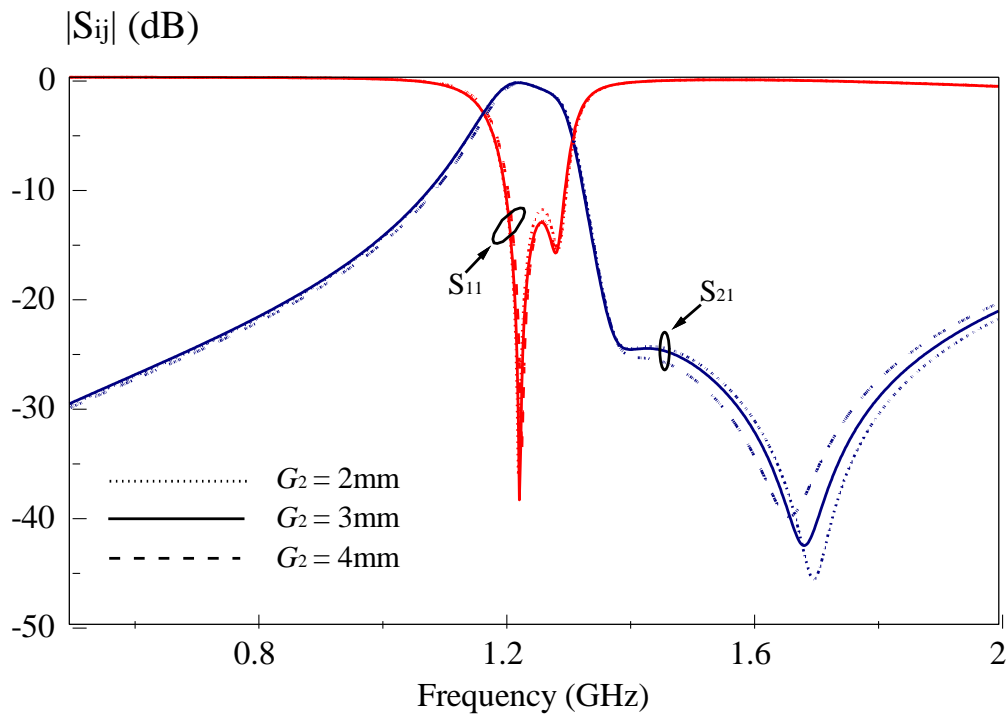


Figure 4.4: Effects of gap g_2 on the slot-based bandpass filter.

Description:

The parameter g_2 does not cause significant effect on the proposed slot-based bandpass filter. It only effect position of the transmission zero at 1.69 GHz. When the value of g_2 increase, the position of the transmission zero has shifts to lower frequency. Inverse, when the value of g_3 decrease, the position of the transmission zero has shifts to higher frequency.

Analysis 3

- Parameter : g_3
- Optimum value : 3 mm
- Step-down value : 2 mm
- Step-up value : 4 mm

Results:

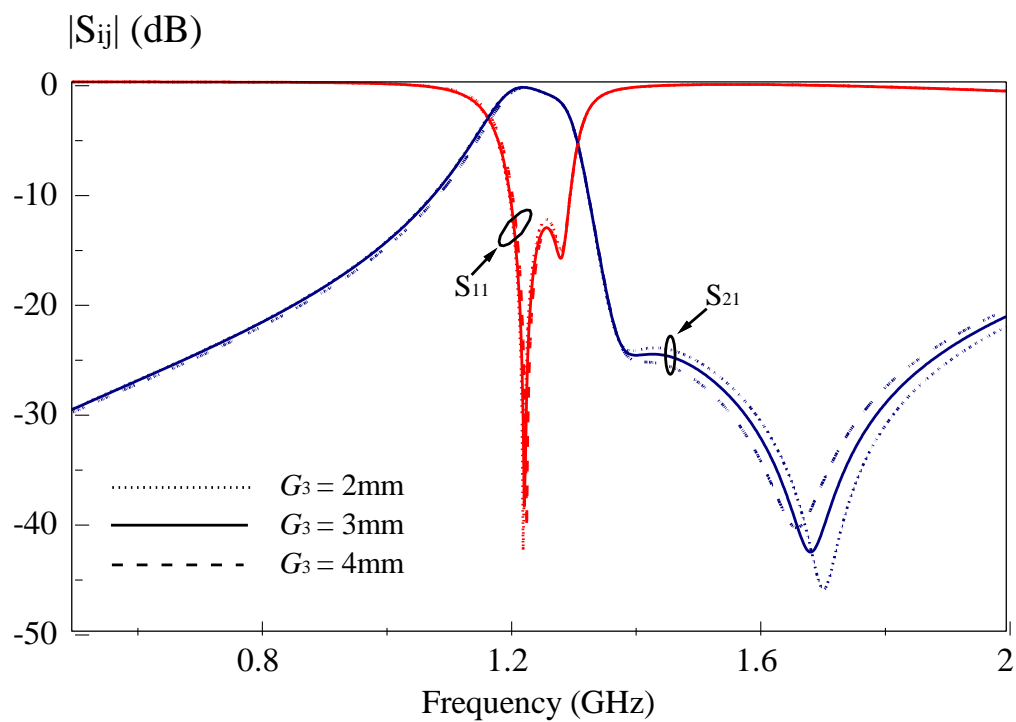


Figure 4.5: Effects of gap g_3 on the slot-based bandpass filter.

Description:

Vary parameter of g_3 does not cause significant effect on the proposed slot-based bandpass filter. The effects when parameter of g_3 altered is almost same like g_2 .

Analysis 4

- Parameter : g_4
- Optimum value : 1.0 mm
- Step-down value : 0.5 mm
- Step-up value : 1.5 mm

Results:

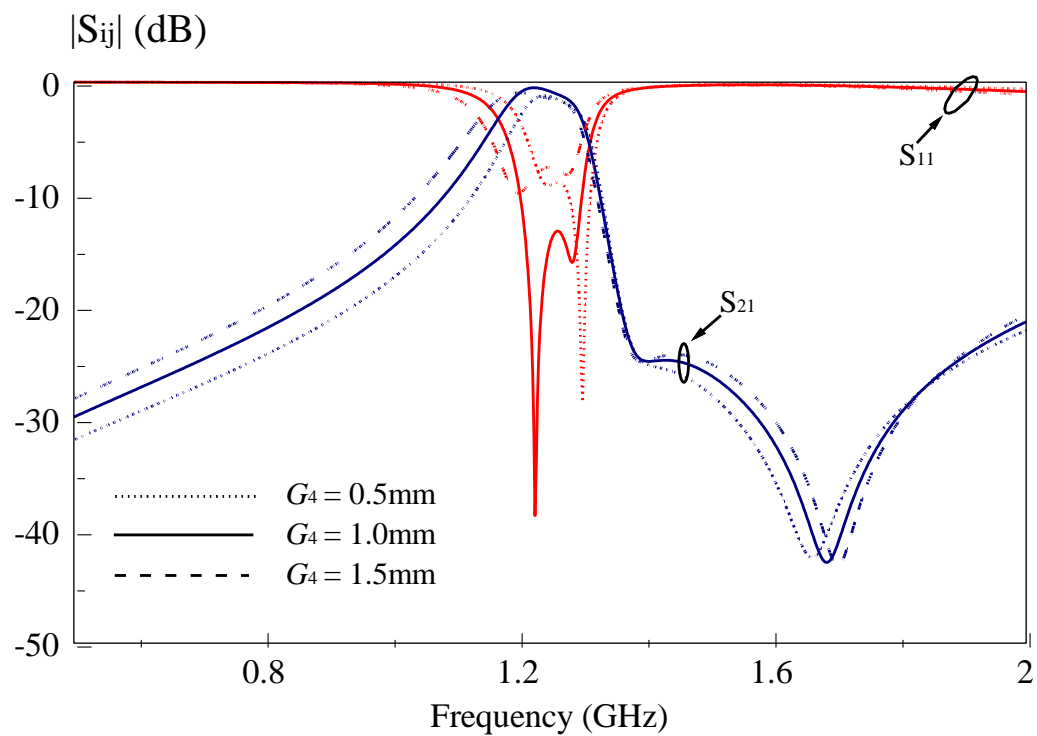


Figure 4.6: Effects of gap g_4 on the slot-based bandpass filter.

Description:

Gap g_4 play an important role in the proposed slot-based bandpass filter. Vary the parameter of g_4 has affect the bandwidth and the return loss of the proposed slot-based bandpass filter. When the gap size become large, the bandwidth of the proposed filter become wide too. However, the return loss of the filter becomes higher.

Analysis 5

- Parameter : g_5
- Optimum value : 1.0 mm
- Step-down value : 0.5 mm
- Step-up value : 1.5 mm
-

Results:

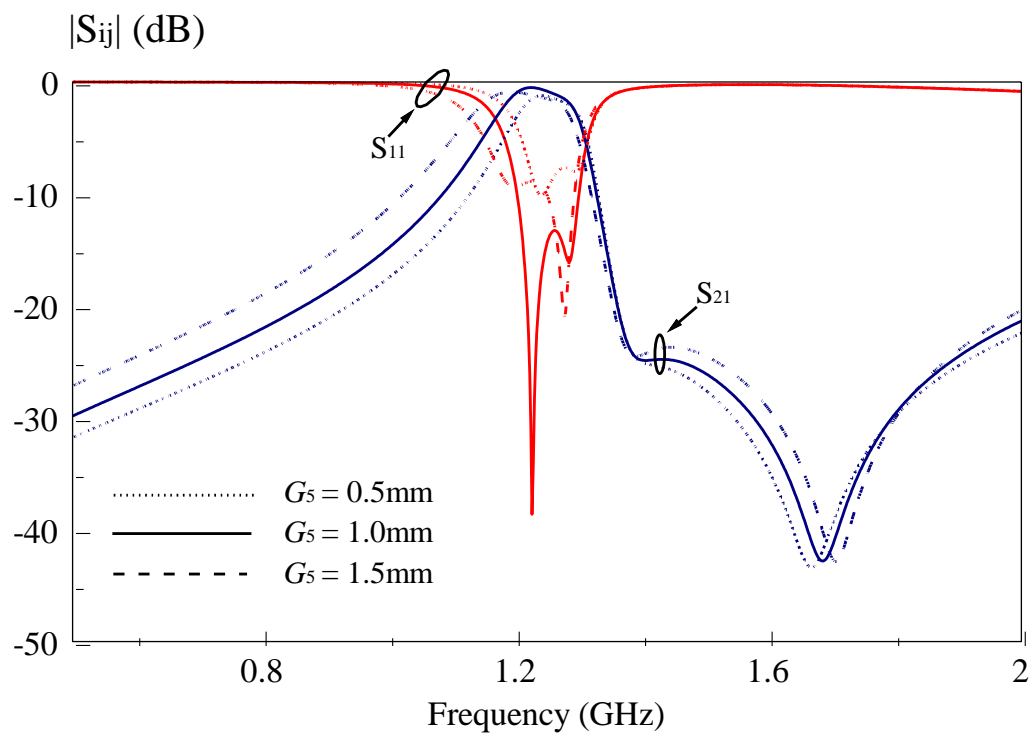


Figure 4.7: Effects of gap g_5 on the slot-based bandpass filter.

Description:

With reference to the amplitude response shown in Figure 4.7, we can clearly see that the gap g_5 significantly affects the bandwidth and the return loss of the proposed filter. Variations in the amplitude response are almost the same as in the g_4 case. The optimum value of g_5 even though the bandwidth of the filter did not widen like 1.5 mm, it has a smaller return loss.

Analysis 6

- Parameter : w_1
- Optimum value : 3.5mm
- Step-down value : 2.5 mm
- Step-up value : 4.5 mm

Results:

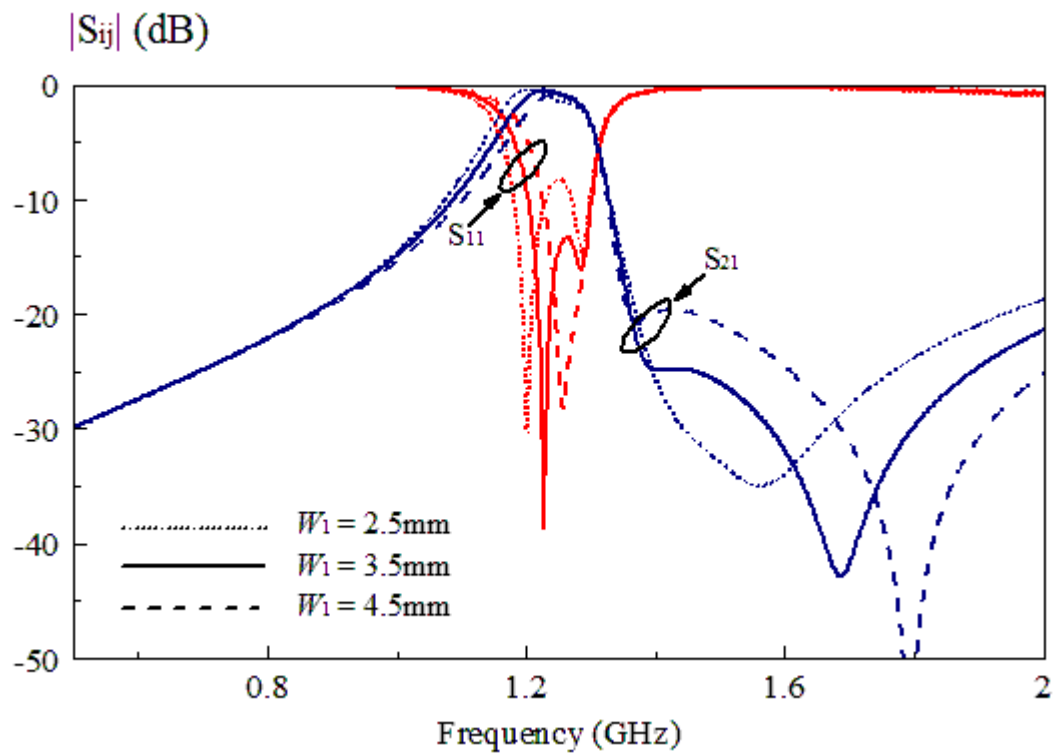


Figure 4.8: Effects of width w_1 on the slot-based bandpass filter.

Description:

Based on the Figure 4.8, the width w_1 of the proposed filter will affect the curve of S_{11} . When the width size is decrease, the curve of S_{11} will slightly shifts to lower frequency and the return loss will increase. Furthermore, the position of the transmission zero also will shift lower. Otherwise, the curve of S_{11} and the position of the transmission zero will shift higher.

Analysis 7

- Parameter : w_2
- Optimum value : 0.50 mm
- Step-down value : 0.25 mm
- Step-up value : 1.00 mm

Results:

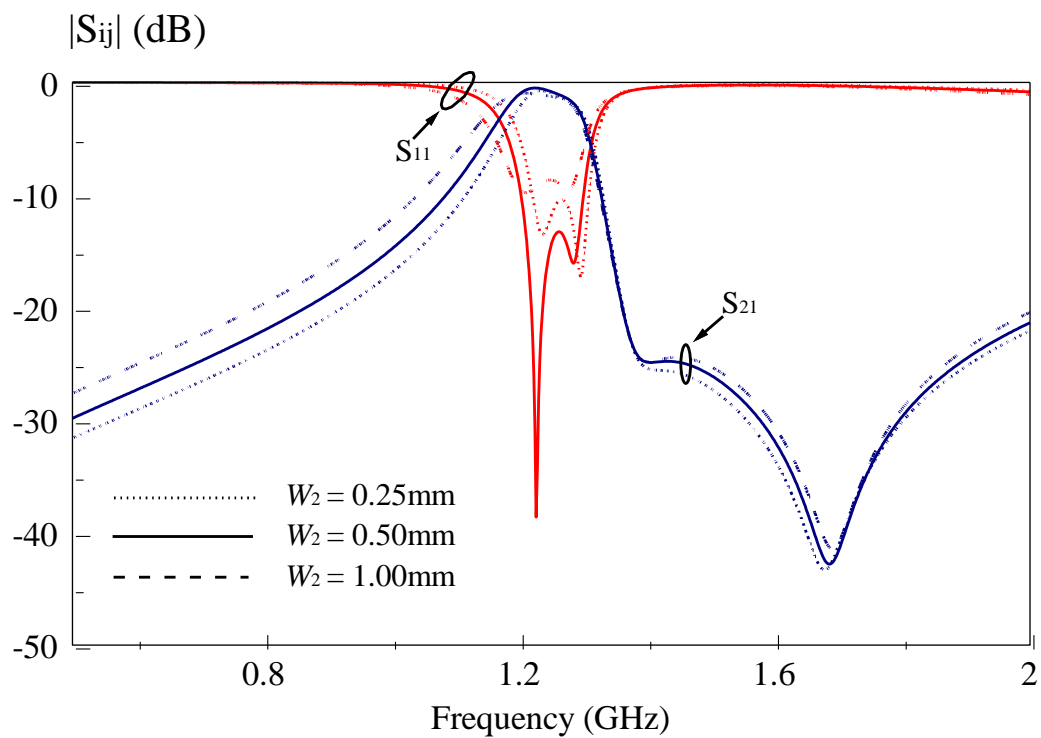


Figure 4.9: Effects of width w_2 on the slot-based bandpass filter.

Description:

In this project, the width w_2 of the proposed BPF is designed to 0.5mm. By changing the value of w_2 , it has affected the bandwidth of the filter. Besides that, it also affected the curve of S_{11} .

Analysis 8

- Parameter : w_3
- Optimum value : 0.50 mm
- Step-down value : 0.25 mm
- Step-up value : 1. mm

Results:

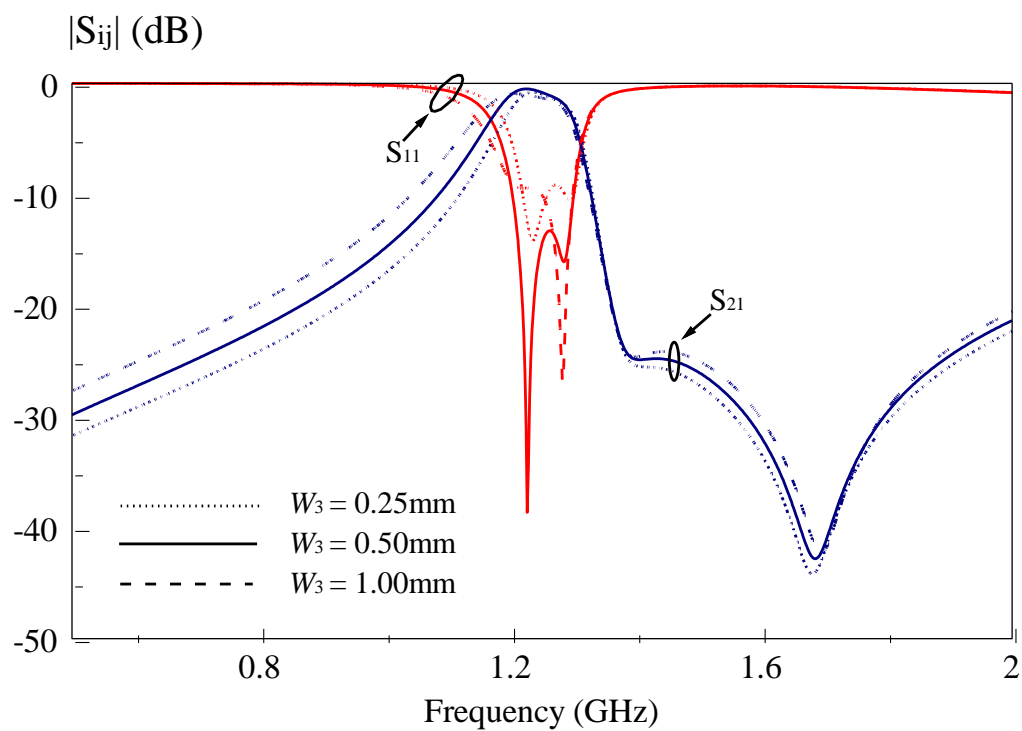


Figure 4.10: Effects of width w_3 on the slot-based bandpass filter.

Description:

As can be seen in the figure 4.10, the width w_3 significant affect the curve of S_{11} and S_{21} . The effects when parameter of w_3 altered is almost same like w_2 .

Analysis 9

- Parameter : d_1
- Optimum value : 15.575 mm
- Step-down value : 13.575 mm
- Step-up value : 17.575 mm

Results:

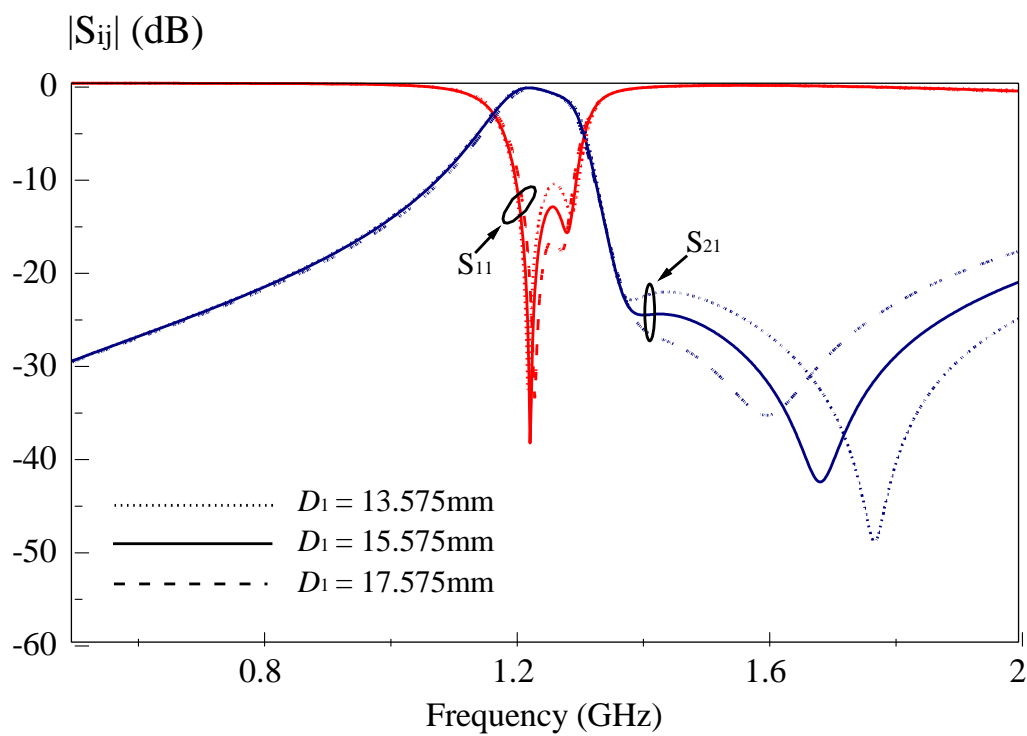


Figure 4.11: Effects of distance d_1 on the slot-based bandpass filter.

Description:

The parameter d_1 does not cause significant effect on the proposed slot-based bandpass filter. It only slightly affects the return loss of the proposed bandpass filter. In addition, the position of the transmission zero also shifted.

Analysis 10

- Parameter : d_2
- Optimum value : 13.075 mm
- Step-down value : 11.075 mm
- Step-up value : 15.075 mm

Results:

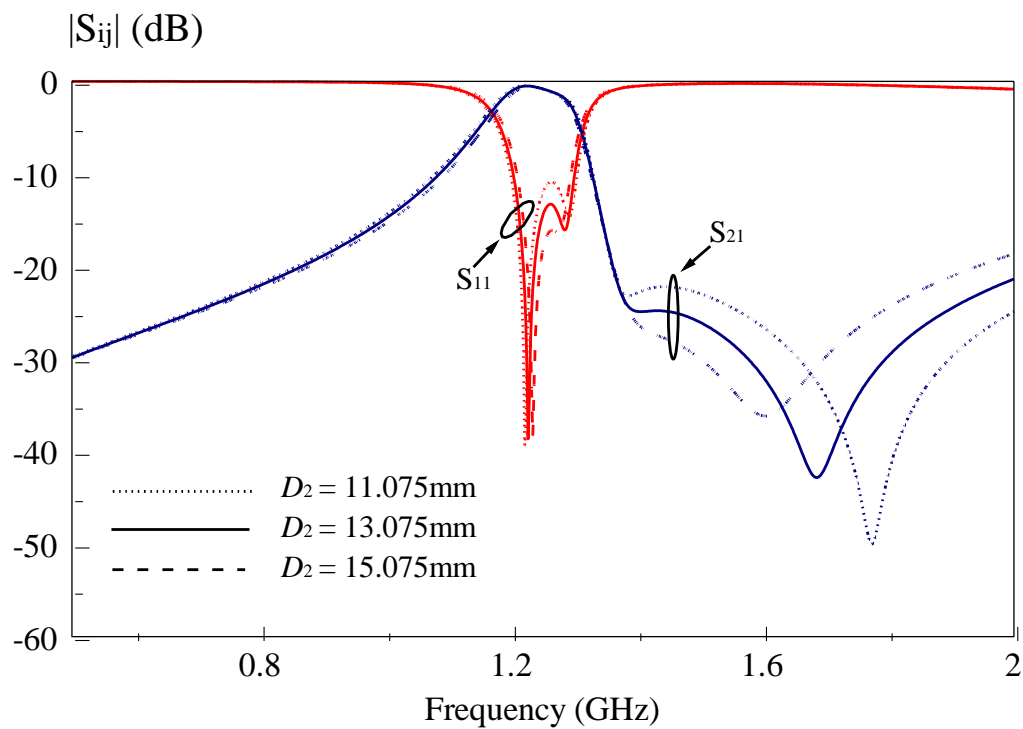


Figure 4.12: Effects of distance d_2 on the slot-based bandpass filter.

Description:

Parameter d_2 has the same effect as that for d_1 . Distance d_2 is the distance between starting point of l_9 and transmission line shown in Figure 4.1. The position of transmission zero shift to lower frequency when the distance d_2 is stepped down but shift to higher frequency when it is stepped up.

Analysis 11

- Parameter : l_1
- Optimum value : 15 mm
- Step-down value : 14 mm
- Step-up value : 16 mm

Results:

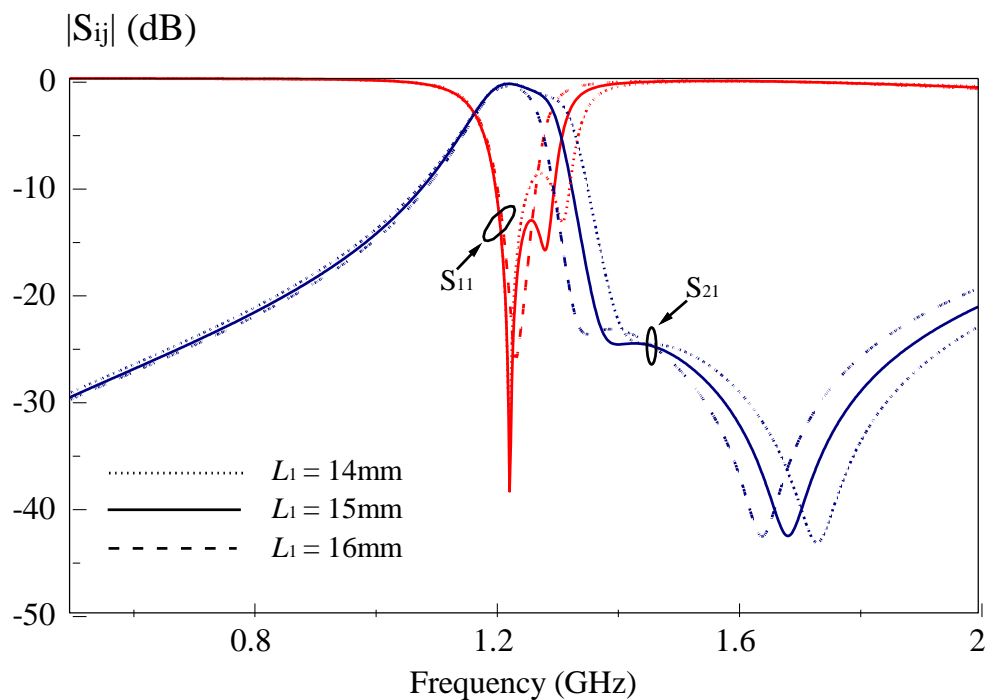


Figure 4.13: Effects of length l_1 on the slot-based bandpass filter.

Description:

The parameter l_1 has affected the bandwidth of the proposed bandpass filter. When the length l_1 is stepped down, bandwidth of the proposed bandpass filter has increase. However, the return loss of BPF has increase too. When the length l_1 is stepped up, the bandwidth of the proposed BPF has decrease. In addition, the position of the transmission zero has slightly shifted when the value of l_1 is change.

Analysis 12

- Parameter : l_2
- Optimum value : 20 mm
- Step-down value : 19 mm
- Step-up value : 21 mm

Results:

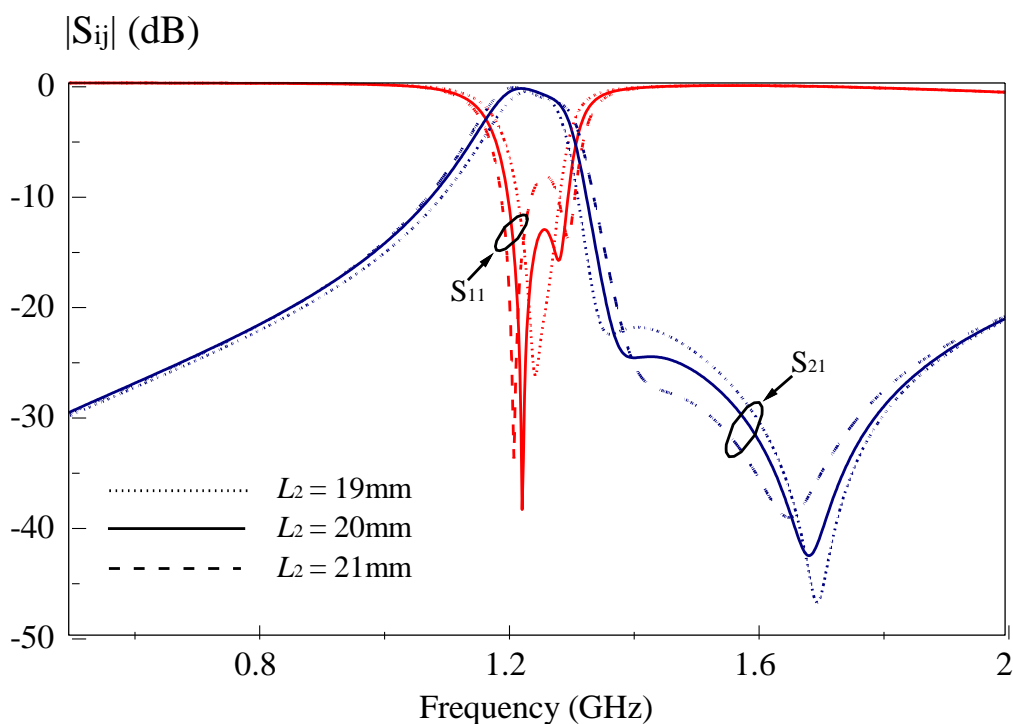


Figure 4.14: Effects of length l_2 on the slot-based bandpass filter.

Description:

From the Figure 4.14, we can clearly see when the length l_2 is change; the curve of S_{11} is varying too. Besides that, the position of transmission zero is also slightly shifted.

Analysis 13

- Parameter : l_3
- Optimum value : 25.0 mm
- Step-down value : 24.0 mm
- Step-up value : 25.5 mm

Results:

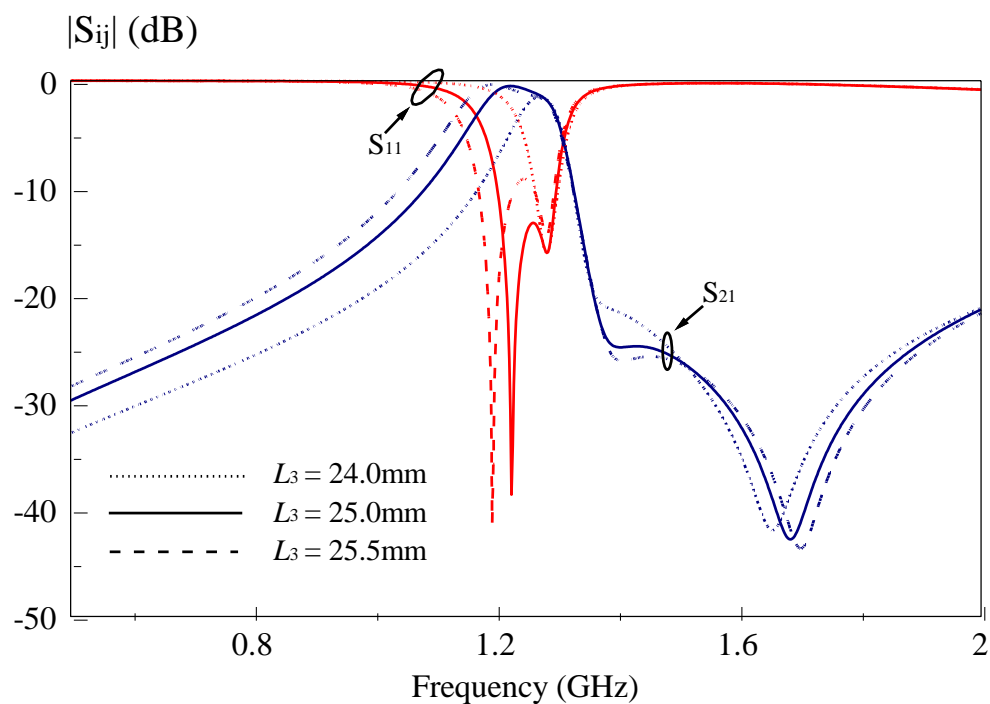


Figure 4.15: Effects of length l_3 on the slot-based bandpass filter.

Description:

The parameter length l_3 affect the operation bandwidth of the proposed slot-based bandpass filter. It becomes wide when l_3 is increase and but smaller when it is decrease. Furthermore, the return loss of bandpass filter also varies when the value of length l_3 is altered.

Analysis 14

- Parameter : l_4
- Optimum value : 30.0 mm
- Step-down value : 29.5 mm
- Step-up value : 31.0 mm

Results:

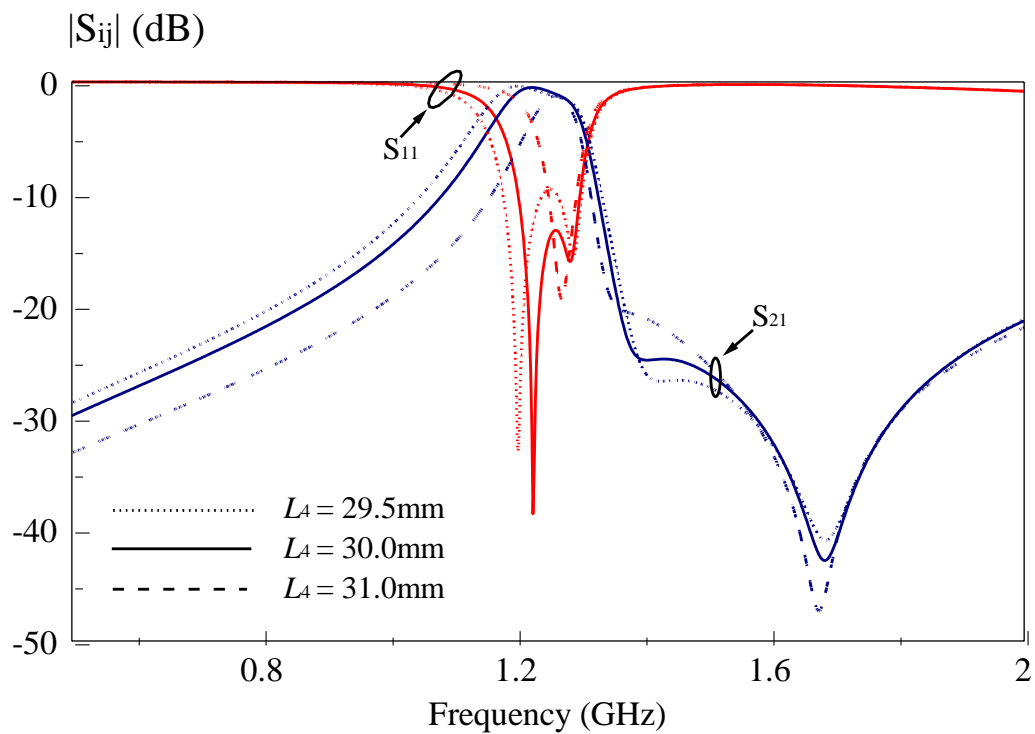


Figure 4.16: Effects of length l_4 on the slot-based bandpass filter.

Description:

By observing the amplitude responses when varying parameter l_4 , we can clearly see that operation bandwidth and the curve of S_{11} are altered. In addition, the effect is opposite to the parameter l_3 . When the value l_4 is increased, the operation bandwidth is reduced. When the value l_4 is decreased, it becomes wider.

Analysis 15

- Parameter : l_5
- Optimum value : 25 mm
- Step-down value : 24 mm
- Step-up value : 26 mm

Results:

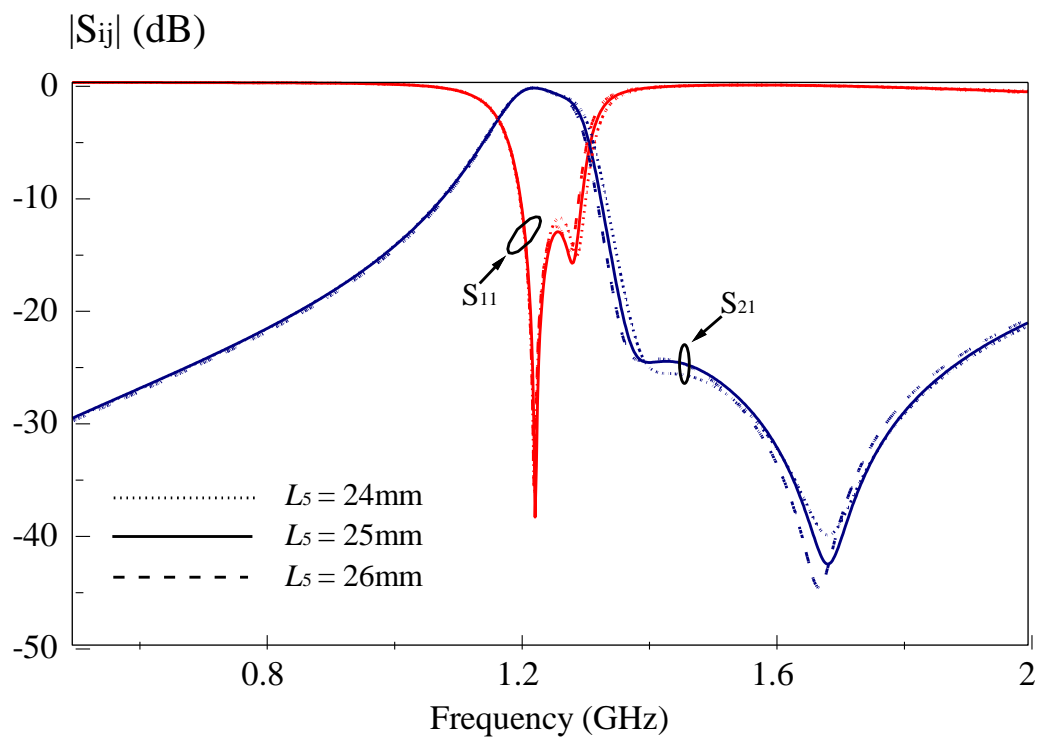


Figure 4.17: Effects of length l_5 on the slot-based bandpass filter.

Description:

From the figure 4.17, we can clearly see the parameter l_5 has no significant effect on the proposed slot-based bandpass filter. There only slight affect the return loss of the bandpass filter. Besides that, transmission zero also slightly shifts when the parameter l_5 is changed.

Analysis 16

- Parameter : l_6
- Optimum value : 32 mm
- Step-down value : 31 mm
- Step-up value : 33 mm

Results:

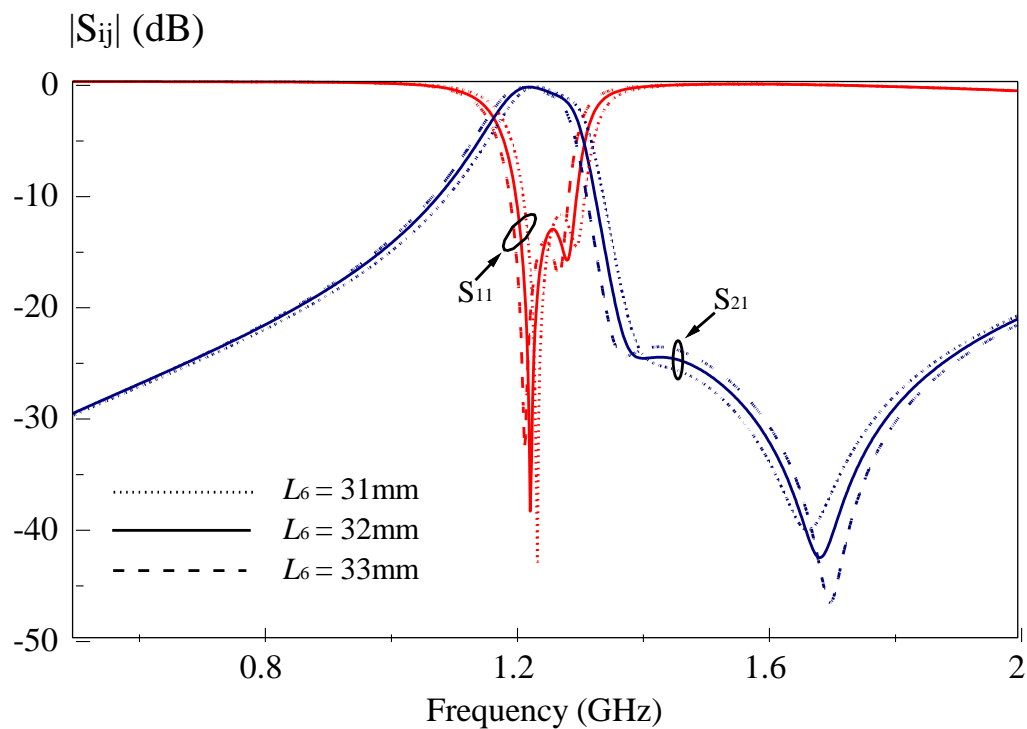


Figure 4.18: Effects of length l_6 on the slot-based bandpass filter.

Description:

Parameter l_6 does not cause much effect when the value of l_6 is changed. Based on the figure 4.18, the bandwidth has increase when the parameter l_6 stepped up but decrease when the parameter l_6 stepped down.

Analysis 17

- Parameter : l_7
- Optimum value : 15 mm
- Step-down value : 14 mm
- Step-up value : 16 mm

Results:

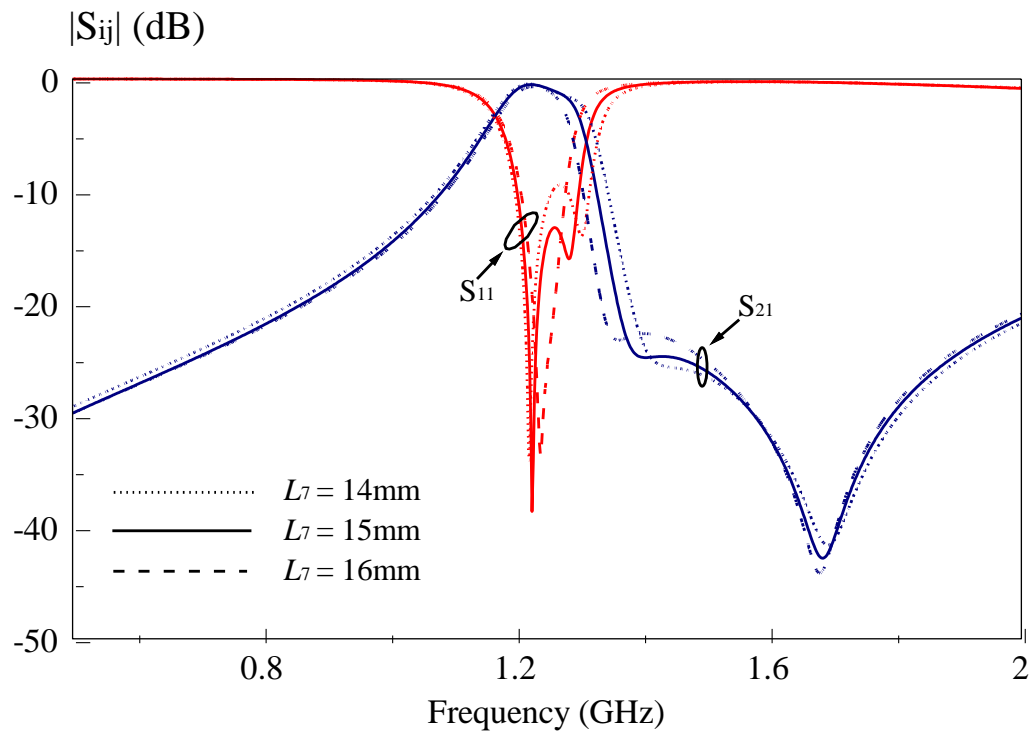


Figure 4.19: Effects of length l_7 on the slot-based bandpass filter.

Description:

Analysis was done for the parameter l_7 and no major effect was found. The position of the transmission zero almost at the same position. Besides that, the operation bandwidth slightly increase when the length l_7 become shorter and decrease when the length l_7 become longer.

Analysis 18

- Parameter : l_8
- Optimum value : 20 mm
- Step-down value : 19 mm
- Step-up value : 21 mm

Results:

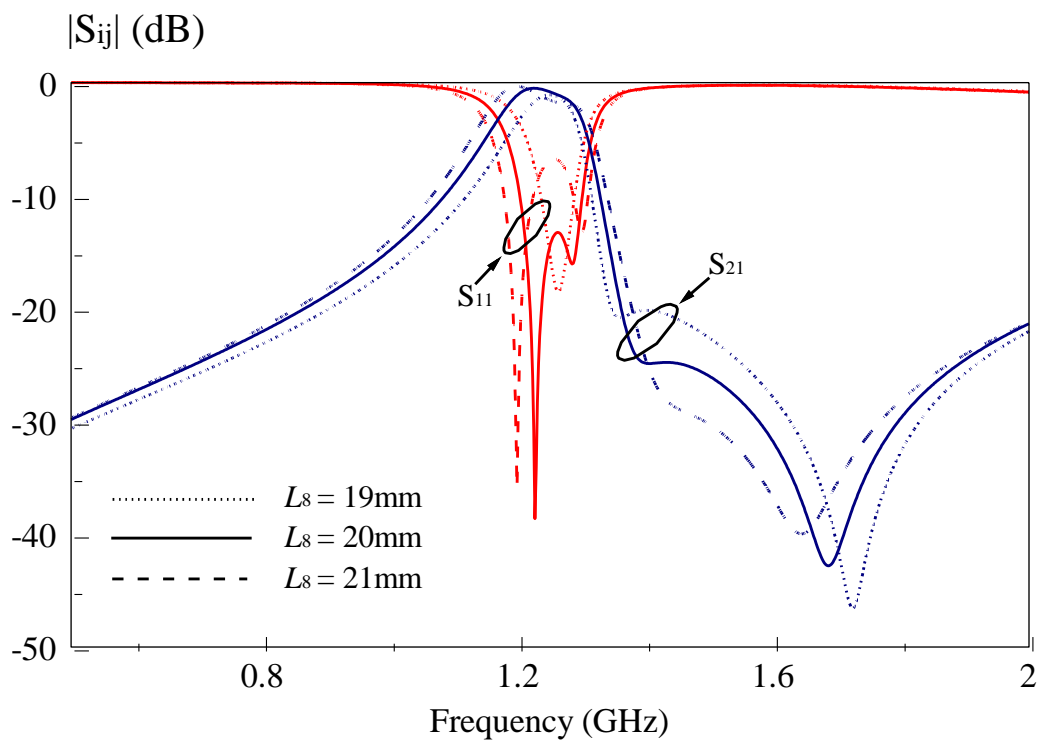


Figure 4.20: Effects of length l_8 on the slot-based bandpass filter.

Description:

From the Figure 4.20, we can clearly see the parameter l_8 plays an important role when designing the proposed bandpass filter. It decides the bandwidth of the device. When l_8 is increase to 20mm, the bandwidth goes widen. On the other hand, it moves smaller for $l_8 = 19$ mm. However, we still need to observe the return loss of the bandpass filter.

Analysis 19

- Parameter : l_9
- Optimum value : 26 mm
- Step-down value : 25 mm
- Step-up value : 27 mm

Results:

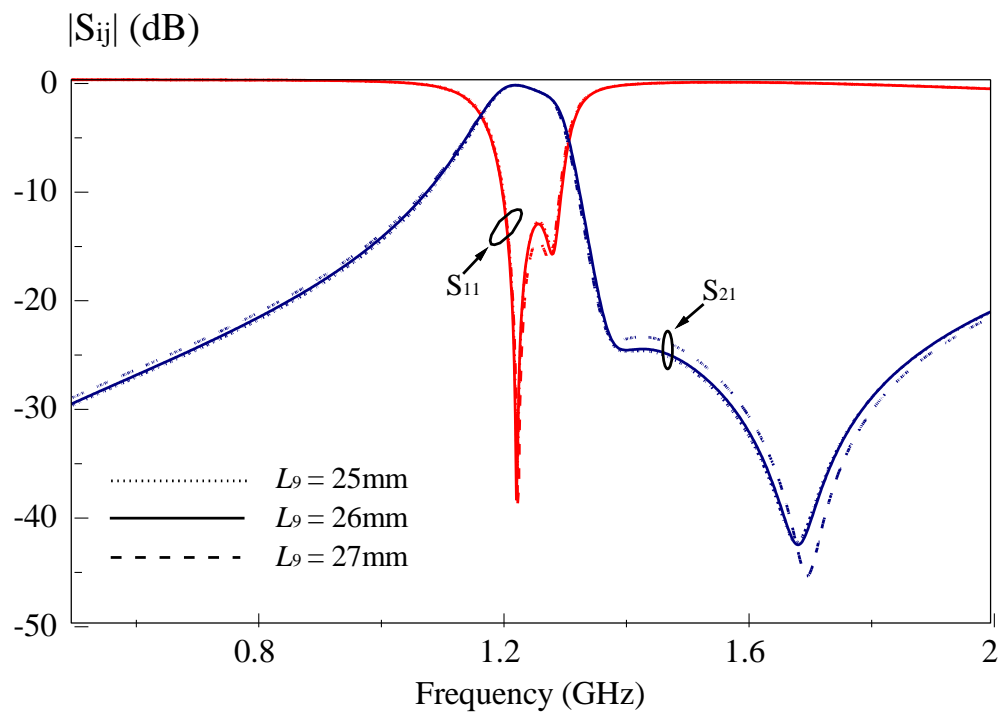


Figure 4.21: Effects of length l_9 on the slot-based bandpass filter.

Description:

According to the figure 4.21, the parameter l_9 does not cause significant effect on the bandpass filter. It only slightly shifts the position of the transmission zero.

Analysis 20

- Parameter : l_{10}
- Optimum value : 26 mm
- Step-down value : 25 mm
- Step-up value : 27 mm

Results:

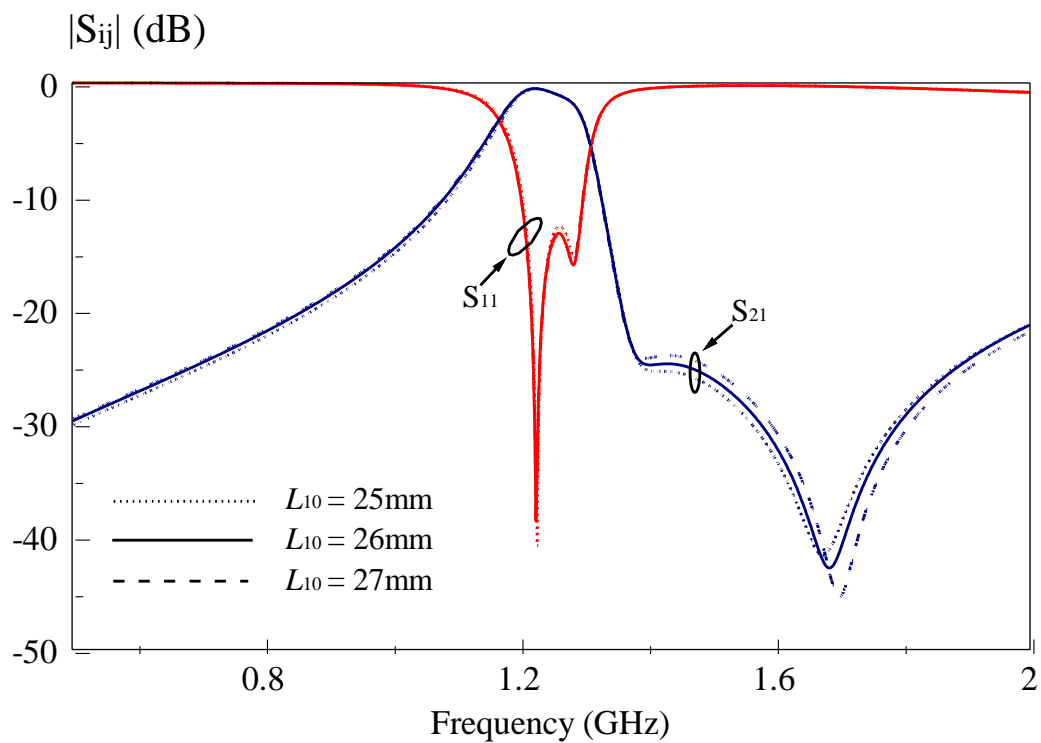


Figure 4.22: Effects of length l_{10} on the slot-based bandpass filter.

Description:

Similarly, the length l_{10} does not have significant effect on the S parameters. The case has almost same like l_9 . The position of transmission zero has slightly shifted when the parameter is altered.

4.5 Discussion

As we know, bandpass filter has widely use in modern world. It is because bandpass filter have many advantages such as smaller size, high selectivity, wide upper stop-band, low insertion loss and cost. Based on the simulated result of the proposed slot-based bandpass filter, it has fulfilled the requirements. The proposed band-pass filter has a smaller size which is $5.6\text{cm} \times 5.6\text{cm}$. It is used FR-4 substrate microstrip circuit board, which is a lower cost material. Furthermore, the proposed bandpass filter has a low insertion loss which is less than 2.77dB from 1.21 to 1.29 GHz, and the minimum insertion loss is only 0.5dB. In addition, the proposed bandpass filter has a smaller return loss which is less than -13dB in the passband.

A slot-based bandpass filter with different design parameters have been analyzed and studied. It can be useful for obtain an optimum slot-based bandpass filter. Based on the parametric analysis in section 3.4, several parameters are found which can significant affect the performance of the proposed bandpass filter such as $g_1, g_4, g_5, w_1, w_2, w_3, l_1, l_2, l_3, l_4, l_7$ and l_8 . They all are the key parameters to design the proposed slot-based bandpass filters.

In this chapter did not include the result section, it is because the author not enough time to fabricate the proposed filter. However, from the simulation result and those parametric analyses, we can observe the proposed filter is can realized.

CHAPTER 5

FUTURE WORK AND RECOMMENDATIONS

5.1 Achievements

In this project, the slot-based directional coupler has been proposed and investigated in the Chapter 3. The proposed idea was demonstrated on the RT Duroid 5870 substrate. The proposed slot-based directional coupler has 10 dB coupling level. Besides that, the proposed idea has lower insertion loss which is less than 4.5dB. It also has lower return loss which is less than -15dB. The measured result is compared with the simulated result.

A slot-based bandpass filter has been proposed and discussed in Chapter 4. Different designed parameter has been analyzed, it easy to design an optimum filter. Some of the issue for the designing the proposed filter has been discussed in Chapter 4.5. In the proposed slot-based bandpass filter, a total bandwidth of 130 MHz was obtained. It has been confirmed that input signal can filter in the passband of the proposed filter.

5.2 Future Work

As for the proposed slot-based directional coupler, coupling level can increase by adjust the gap of the coupled line. It can cause the operation bandwidth become wider. Therefore, as for future improvement, the coupled level can improve by adjust several design parameters. Besides that, the etching process need to be careful during fabricated the proposed design. This is because, over etching will affect the result accurate even change the result. For second proposed idea in Chapter 4, the operation bandwidth can improve by adjust the gap size and length size. Furthermore, the proposed filter can demonstrate on microstrip board. Comparison between measured and simulated result can be made.

5.3 Conclusion

Both the slot-based directional coupler and slot-based bandpass filter have been designed. Demonstrated the proposed design can been made to ensure the agreement between simulation and measured results. In this thesis, the design considerations and issues of the proposed directional coupler and filter have also been studied. The objectives of this project have been met.

REFERENCES

Amin M. Abbosh and Marek E. Bialkowski. (February 2007). Design of Compact Directional Couplers for UWB Applications. *IEEE Transaction on Microwave Theory and Techniques* , Vol. 55, No. 2.

Chang, K. *RF and Microwave Wireless System*. New York/ Chichester/ Weinheim/ Brisbane/ Singapore/ Toronto: John Wiley & Sons, Inc.

C. -L. Wei, B. -F. Jia, Z. -J. Zhu, M. -C. Tang. (October 2010). Novel trigonal dual-mode filter with controllable transmission zeros. *IET Microwaves, Antennas & Propagation*.

Directional Couplers. (n.d.). Retrieved March 5, 2012, from Microwave Encyclopedia: www.microwaves101.com/encyclopedia/directionalcouplers.cfm

Dr. Otman El Mrabet. (2006). High Frequency Structure Simulator (HFSS) Tutorial. France. Retrieved August, 25, 2012, from http://morteza.rezaee.student.um.ac.ir/imagesm/6446/stories/e-books/hfss/tutorial_antenna.pdf.

Dydyk, M. (1999). Microstrip Directional Couplers with Ideal Performance via Single-Element Compensation. *IEEE Transaction on Microwave Theory and Techniques* , vol 47, No.6.

Han, L. (Dec 2011). A design method of microstrip directional coupler with multi-element compensation. *IEEE International Symposium on Radio Frequency Integration Technology* .

Hee-Ran Ahn, Bumman Kim. (Oct 2006). Transmission-Line Directional Couplers for Impedance Transforming. *IEEE Microwave and Wireless Components Letters*, vol 16, No. 10.

Hong J. S. & M.J. Lancaster. . (2001). *Microstrip Filter for RF/Microwave Applications*. New York/ Chichester/ Weinheim/ Brisbane/ Singapore/ Toronto: John Wiley & Sons, Inc.

James Richardson. (2012). Microwave Radio Frequencies. Global Warming and Microwave. Retrieved August 23, 2012, from <http://globalmicrowave.org/microwaves.php>.

J.K. Shimizu, E. M. T. Jones. (1958). Coupled-Transmission-Line Directional Coupler. *IEEE Transactions on Microwave Theory and Techniques* , 404.

J-L. Li, S.-W Qu and Q. Xue. (February 2007). Microstrip directional coupler with flat coupling and high isolation. *Electronic Letters* , Vol. 43, No. 4.

Johannes Muller, Minh N. Pham and Arne F. Jacob. (n.d.). Directional Coupler Compensation with Optimally Positioned Capacitances. *IEEE transaction on Microwave Theory and Techniques* .

Kaixue Ma, Keith Chock Boon Liang, Rajanik Mark Jayasuriya, Kiat Seng Yeo. (Jan 2009). A wideband and high rejection multimode bandpass filter using stub perturbation. *IEEE on Microwave and Wireless Components Letter* , vol 19, no.1, pages 24-26.

M.Chudzik, I. Arnedo, A. Lujambio, I. Arregui, F. Teberio, M.A.G. Laso and T.Lopetegi. (November 2011). Microstrip coupled-line directional coupler with enhanced coupling based on EBG concept. *Electronic Letters* , Vol 47, No. 23.

Pozar, D. M. (Jan 1985). Microstrip antenna aperture-coupled to a microstripline. *Electronic Letter* , vol. 21, no. 2, pp. 49 - 50.

Pozar, D. M. (1998). *Microwave Engineering* . Canada: John Wiley & Sons, Inc.

Ravee Phromloungsri, Mitchai Chongcheawchamnan, Ian D. Robertson. (2006). Inductively compensated parallel coupled microstrip lines and their applications. *IEEE transaction on Microwave Theory and Techniques* , Vol. 54, No.9.

Seungku Lee, Yongshik Lee. (April 2010). A Design Method for Microstrip Directional Couplers Loaded With Shunt Inductors for Directivity Enhancement. *IEEE Transactions on Microwave Theory and Techniques* , Vol. 58, No.4.

T. Jensen, V. Zhurbenko, V. Krozer, and P. Meincke. (Dec. 2007). Coupled transmission lines as impedance transformer. *IEEE transaction on Microwave Theory and Techniques* , vol 55, no. 12, pages 2957-2965.

Toshiaki Tanaka, Kikuo Tsunoda, Masayoshi Aikawa. (Dec. 1988). Slot-Coupled Directional Couplers Between Double-Side Substrate Microstrip Lines and Their Applications. *IEEE transaction on Microwave Theory and Techniques*, vol 36, no. 12.

Wayne Storr. (2012, August). Band Pass Filter. Retrieved August 24, 2012, from http://www.electronics-tutorials.ws/filter/filter_4.html.

Wenming Li, Haiwen Liu, Xiaohua Li, Ahmed Boutejdar, Shuxin Wang, Fu Tong. (2008). Novel Microstrip Bandpass Filter With Slotted Hexagonal Resonators And Capacitive Loading. *IEEE Microwave Conference*.

Werner A. Arriola, Jae Young Lee, and Ihn Seok Kim. (2011). Wideband 3 dB Branch Line Coupler Based on $\lambda/4$ Open Circuited Coupled-lines. *IEEE Microwave and Wireless Components Letters* .

Wikipedia. (2012, August 15). Band-pass filter. Retrieved August 22, 2012, from http://en.wikipedia.org/wiki/Band-pass_filter.

Wikipedia. (2012, August 23). Microwave. Retrieved August 24, 2012, from <http://en.wikipedia.org/wiki/Microwave>.

Wikipedia. (2012, May 7). Power dividers and directional couplers. Retrieved August 24, 2012, from http://en.wikipedia.org/wiki/Power_dividers_and_directional_couplers.

Xi Wang, Wen-Yan Yin and Ke-Li Wu. (2011). A Dual Band Coupled-Line Coupler with an Arbitrary Coupling Coefficient. *IEEE transacton on Microwave Theory and Techniques* .